

MODELING OF BURNING OIL ON
A WATER SURFACE

John J. Anthony Jr.

MODELING OF BURNING OIL ON A WATER SURFACE

by

JOHN J. ANTHONY JR.

Lieutenant (j.g.), United States Coast Guard

B.S., United States Coast Guard Academy

(1973)

SUBMITTED IN PARTIAL FULFILLMENT
OF THE REQUIREMENTS FOR THE
DEGREES OF

OCEAN ENGINEER

and

[M. S.]

S.M. MECHANICAL ENGINEERING

at the

MASSACHUSETTS INSTITUTE OF TECHNOLOGY

MAY 1977

MODELING OF BURNING OIL ON A WATER SURFACE

by

JOHN J. ANTHONY JR.

Submitted to the Department of Ocean Engineering
on May 12, 1977 in partial fulfillment of the requirements
for the Degree of Ocean Engineer and S.M Mechanical Engineering

ABSTRACT

With the great concern over large accidental spills of oil on to the high seas and in harbors, it has become imperative that effective oil cleanup measures be developed to prevent the excessive damage to the waters and coast which might otherwise occur. Burning the spilled oil has been proposed as an efficient and relatively non-polluting means by which to accomplish this task. The heat transfer associated with burning has been examined for oils in general and for oils burning on water in particular. A model which accounts for the effects of diverse oil compositions and the water sublayer has been developed and predicted results are compared with the experimental data presently available. On this basis the model has been judged to have useful potential in the analysis of this method of oil spill cleanup. Tentative conclusions on the application of the model to the work currently being performed with burning agents are included as well.

Thesis supervisor: James A. Fay
Professor of Mechanical Engineering

Acknowledgements

The author expresses his deep thanks and appreciation to Professor James A. Fay whose guidance and patience were instrumental to the successful completion of this thesis. Additional gratitude goes to Miss Debby Freedman for masterfully typing the finished work.

Table of Contents

Introduction	5
Chapter 1 -- Burning Rates	8
Chapter 2 -- Temperature Distributions	20
Chapter 3 -- Effects of Oil Composition on Burning	31
Chapter 4 -- Effects of the Water Sublayer	55
Chapter 5 -- Application of Model to Real Burns	70
Conclusions	74
Appendix A -- Development of the Binary Boiling Curves	76
Appendix B -- Determining the Depth at Which Boiling Begins in a Burning Binary Solution	81
Appendix C -- Pertinent Properties of Some Petroleum Products	87
Appendix D -- Tabulation of Some Fractionation Data	88
List of Symbols	89
References	92
Bibliography	94

Introduction

Increased interest and concern over the adverse effects of accidental discharges of oil in our harbors and coastal regions has stimulated legislators, scientists and environmentalists to propose solutions to (1) prevent oil spills from occurring and (2) clean up spilled oil as quickly and effectively as possible. As a result of this activity, commercial carriers of petroleum are now liable for every drop of oil that falls to the water. Yet severe penalties and tough legislation cannot prevent the accidental groundings and collisions that will beset some of the world's fleet of tankers every year. To combat the large spills which occur in such instances and minimize their environmental impact, an effective cleanup program must exist.

One of the proposed cleanup methods is to burn the oil that lies on top of the water after an accidental spill or discharge. This method was first attempted on a large scale when the Torrey Canyon spilled a total of 50,000 tons of Kuwait crude oil after grounding off the coast of England in 1967. The only oil burned was that remaining in the ships tanks since the oil spilled on the sea had drifted for four days and was well emulsified before any burning activity was contemplated [22]. Application of burning agents in the form of "Seabeads" was attempted in a spill of Bunker C from the Arrow in 1970 off the coast of Nova Scotia. This venture had limited success as nearly 50% of all the oil on the sea was consumed by burning [22]. Since that time, the Navy, Coast Guard, EPA and several private firms have experimented with a variety of oil burning techniques. The marginal success which

these efforts have had has made oil burning as a cleanup option somewhat less attractive. The emphasis recently has been on further development of burning agents. Some of these agents were used on the spill from the Argo Merchant in 1976 but with little success. Somewhat more successful was the Coast Guard's application of a burning agent to a spill of fuel oil in Buzzards Bay in January 1977. Here about one half of a small 2000 gallon spill was consumed by fire.

Despite these numerous successes and failures, there has been no evidence of any attempt to quantify and establish a model for the mechanism by which oil is burned and in particular, how it burns on water. The existence of such a model would give more direction to the research being conducted in this field. But the subject of course is by no means simple. Oils are complex substances in themselves, but when aspects of the water environment are imposed, an overall approach to the problem must include many elements of fluid mechanics, chemistry and heat transfer. This thesis deals primarily with the heat transfer that takes place in burning oil.

Some previous work on this subject has been accomplished by a number of fire research and fire prevention interests, the emphasis being directed toward prevention and extinguishment of oil fires. Specifically, experiments have centered around obtaining data from pool oil fires in large open tanks with considerable depths of oil. But since in most instances it is only very thin layers near the surface of the oil that are heated and vaporized, some results from these experiments may be applicable to the problem of thin oil layers

burning on water. Despite the nature of the available data, a model for some aspects of burning oil has been accomplished and where it seemed appropriate, reported data was compared to the analytical results. The subsequent model is consistent to the basic precepts of heat transfer and in large part to the data reported by numerous investigators.

The presentation of this model begins in Chapter 1 with the development of some empirical relations for linear burning rates. This is followed in Chapter 2 by an analysis of the temperature distributions in unconfined burning oil, burning oil in tanks, and burning oil on water. Chapter 3 examines the nature of complex solutions and applies the results to oils that consist of high and low boiling point fractions. Utilizing the results of Chapters 1 and 2, a model is developed for determining the thicknesses over which vaporization occurs in complex oils. The first three chapters provide the necessary background to undertake an analysis of oil burning on top of water in Chapter 4. Following a preliminary section on oil thicknesses that result from spreading on water, this chapter analyzes the heat transfer that takes place during burning. Water presence affects burning rate while water that is boiling under a layer of burning oil affects both burning rate and the thickness of oil that will remain after flame extinguishment. Chapter 5 concludes this thesis with some thoughts on how the oil thicknesses which are predicted by the developed model might relate to the use of burning agents or to fires of low flame height.

Chapter 1

Burning Rates

1. Heat transfer to the oil

Free burning liquid petroleum or some other combustible liquid generates heat as a result of the exothermic reaction of the very top layer of fuel with the oxygen in the ambient air. The fraction of this heat which can be transferred to the environment is strictly a function of the rate at which fuel is consumed and the size of the fire. The mass burning rate of the liquid in turn depends on how much heat can be transferred to its surface. A widely quoted work on the size of fires is Thomas' paper, "The Size of Flames from Natural Fires" [1] in which he develops an empirical relation between flame height and pool diameter with mass burning rate as a variable. This relation for liquid fuels is:

$$\frac{L}{d} = 42 \left[\frac{m}{\rho_a \sqrt{gd}} \right]^{0.61} \quad (1-1)$$

In this expression, L is the flame length or height, m is the mass burning rate per unit area, ρ_a the air density at ambient temperature and g is the gravitational acceleration. The diameter of the pool, d , is usually defined as:

$$d = 4x \frac{\text{Area of pool}}{\text{Perimeter of pool}}$$

Although larger fires will be capable of transferring larger amounts of heat the amount of heat transferred to the fuel surface depends on

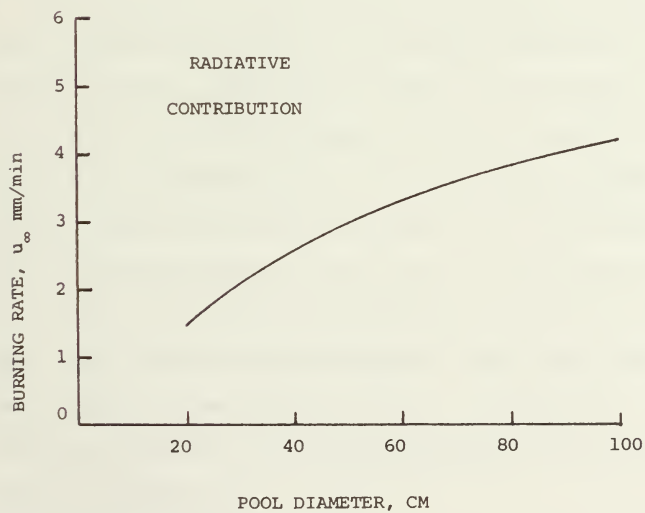
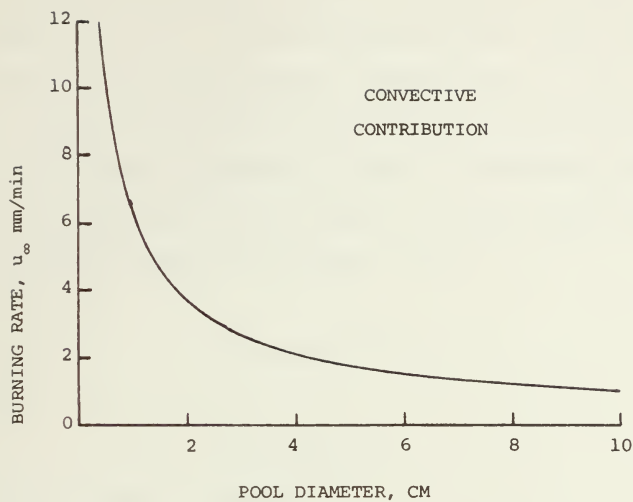
considerations other than flame length.

In his review, Hottel [2] reports on the work of Blinov and Khudiakov [2] and proposes the following equation to predict heat transfer to the surface from the flames:

$$q_s = \frac{\lambda(T_f - T_b)}{d} + U(T_f - T_b) + \sigma F(T_f^4 - T_b^4)(1 - e^{-\kappa d}) \quad (1-2)$$

Here λ is the fuel's thermal conductivity, U is a heat transfer coefficient for convection, σ is the Stefan-Boltzmann constant, and F is the view factor between the flame and the surface. The term $(1 - e^{-\kappa d})$ is the opacity factor; κ is a constant relating to emissivity [3]. For all terms T_f and T_b are the flame temperature and liquid boiling temperature respectively, the assumption being that the burning surface must be at the boiling point in order to vaporize the fuel.

A conduction term is present in equation 1-2 since in this analysis the fuel is confined to some sort of container and there is some conduction through the lips of the container. Though the presence of a container creates additional problems which will be addressed later, it is sufficient at this point to recognize that some conduction is present although it is significant at only the smallest diameters. For the case of an uncontained fire the first term is absent. Luminous flames sweeping back and forth across the fuel surface give rise to the convection term. Figure 1-1 shows that this effect also decreases with an increase in diameter as observed by Blinov [4]



Source is Reference 3

Figure 1-1

and Burgess [3], becoming noticeably less apparent at diameters greater than 10 cm. The only remaining term for large diameters is that for radiation and this has a limiting value as $(1-e^{-\kappa d})$ approaches 1. The heat flux for large fires is therefore governed chiefly by radiation which is asymptotic in nature. Since the heat received goes to heat and vaporize the fuel prior to burning the mass burning rate must also be asymptotic in diameter. Thus,

$$m = m_{\infty}(1-e^{-\kappa d}) = \rho u \quad (1-3)$$

or

$$u = u_{\infty}(1-e^{-\kappa d}) \quad (1-4)$$

when one divides by density.

The velocity u is termed the linear regression rate and is the speed at which the top surface of the burning fuel moves in the downward direction. Experiments by Blinov [4] and Burgess [3] confirm this relation for the fuels tested.* In truth, equations 1-2 and 1-4 may be an oversimplification of the heat transfer process and its effects. Burgess and Hertzberg[3] report that in large fires of alcohol, radiation accounts for only 25% of the total heat transferred; the balance being attributed to convection, though not the flame sweep type of convection mentioned above. This is most likely a feature of fuels whose flames burn with a low luminosity. Despite this modeling conflict, their linear regression rates still vary as stated in equation 1-4.

*With the exception of hydrogen [3]

2. Determination of burning rates

Theoretically, if the flame temperature were known and the view factor could be computed, the limiting regression rate, u_{∞} , could be computed for any fuel. Unfortunately, vagaries in the way different fuels burn do not permit such precise analyses. As a result, the only source of reliable data comes via experimentation. Experimental results are available for a small number of fuels and are reported in references 2 through 8. Data taken by Burgess [3] is displayed in Figure 1-2. In other experiments the variety of types and sizes of containers used makes interpretation of the data difficult. In cases where the results were judged to be reasonable these data were plotted and extrapolated to large diameters to obtain a close approximation of u_{∞} . The results of this work appear in Table 1-1.

There has been only one significant attempt to correlate the limiting regression rate with physical parameters. Burgess [3] was able to fit a straight line to the measured limiting regression rates when they were plotted against H_C/H_V , as depicted in Figure 1-3. H_C is the net heat of combustion and H_V is the sensible heat of vaporization defined as

$$H_V = h_V + c_p (T_b - T_a) \quad (1-5)$$

H_V is actually the heat received by the fuel, q_s , h_V is the latent heat of vaporization, c_p is the specific heat of the fuel and $T_b - T_a$ is the difference between the boiling and ambient, or initial, temperature. The equation for this line is [3]

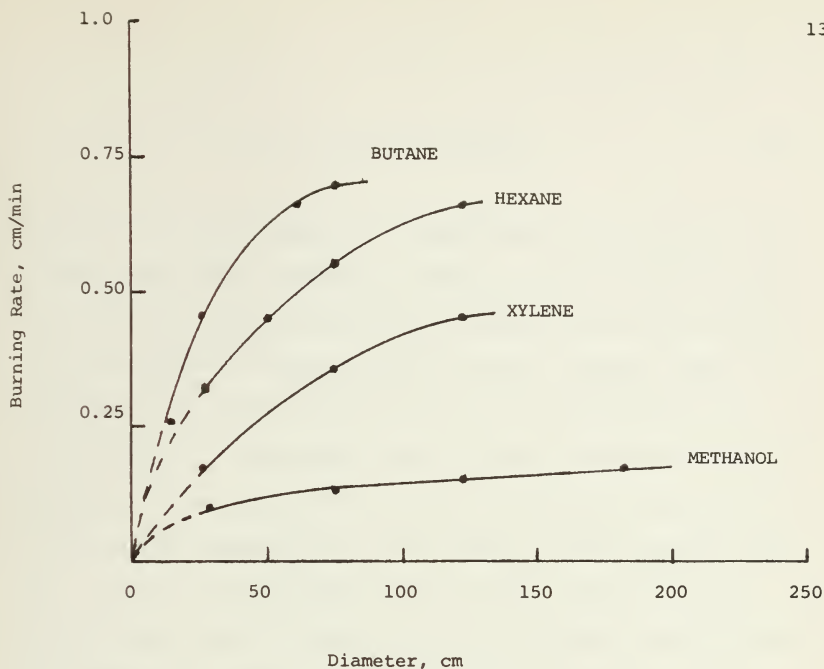


Figure 1-2

TABLE 1-1

Limiting Regression Rates From Extrapolation of Data

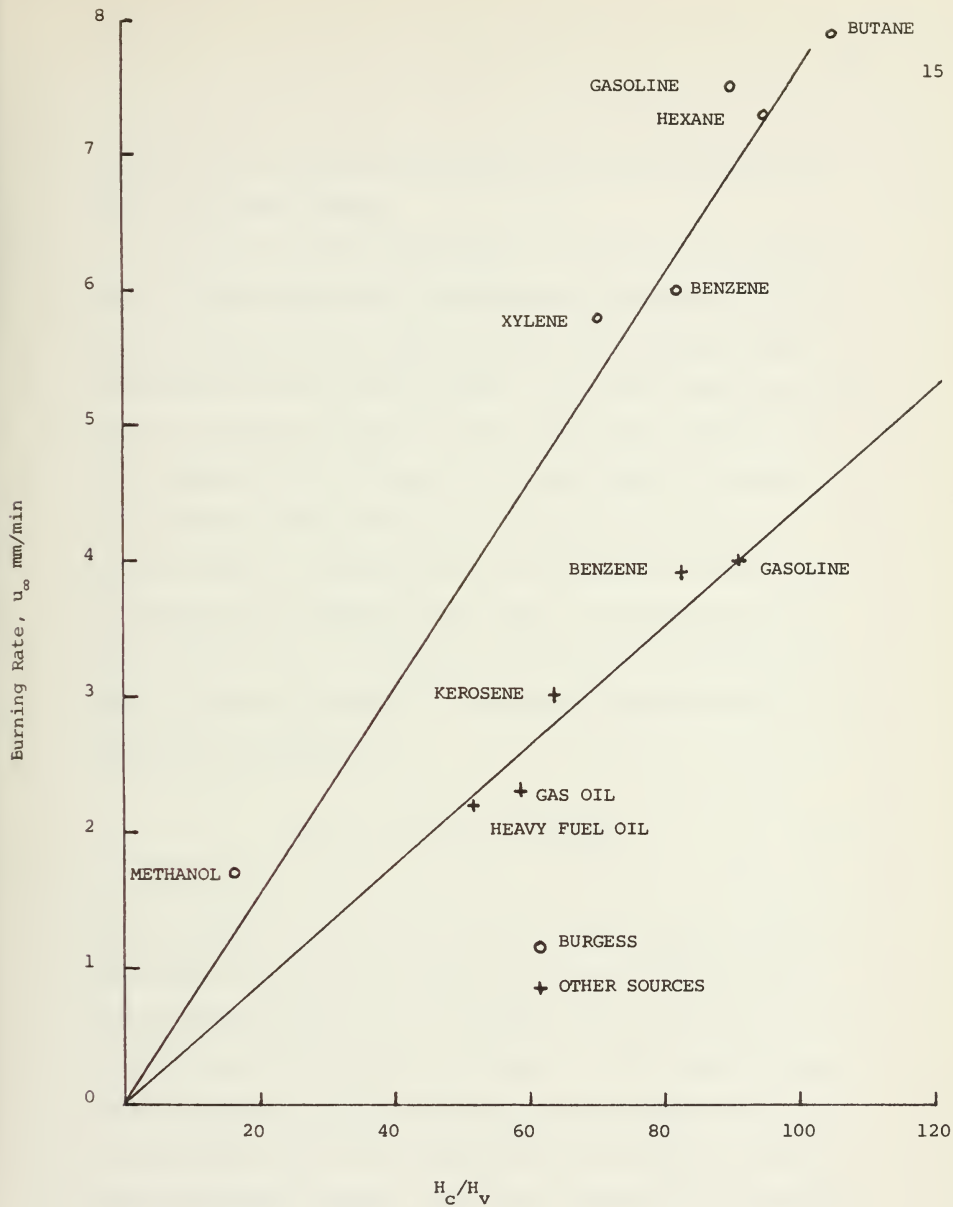
<u>Substance</u>	u_{∞} <u>mm/min</u>	<u>Source</u>
Diethyl ether	6.2	4
Gasoline	4.6	4
	4.3	5
	4.0	4
Tractor Kerosene	4.2	4
Benzene	3.9	6
Diesel Oil	3.6	4
Kerosene	3.0	4
Gas Oil	2.3	8
Heavy Fuel Oil	2.2	4
Vaporizing Oil	2.0	8
Lube Oil #20	1.6	8
Crude Petroleum	1.6	4
Acetone	1.5	5
	1.3	4
Butanol	1.0	4
Methanol	1.0	4,5,6

$$u_{\infty} = 0.076 H_c/H_v \quad (\text{mm/min}) \quad (1-6)$$

Though this relation supports the expectation that a substance which requires more heat to vaporize it before it will burn will naturally burn slower, no physical model can be proposed which would rationalize the existence of this particular relation. However, Burgess has developed some degree of support for a curve of mass burning rate, ρu_{∞} , vs. H_c/H_v . This model*, which is based on radiative transfer, predicts a slope less than but close to that obtained from a plot of the data when reasonable values are assumed for the radiative transfer. Figure 1-3 also contains some data taken from other sources. It is significant that all these values of u_{∞} lie below those that would be predicted by equation 1-6. Much of this discrepancy can be explained by differences in experimental techniques but what cannot be ignored is that the values appear to fall on another line, this one of slope 0.044 mm/min.

The linear relationship between mass burning rate or regression rate and H_c/H_v appears then to be sound. Burgess' slope of 0.076 mm/min appears to be the upper bound as no other source can supply values higher than his. It could also be that a different curve exists for fuels of substantially higher molecular weight. The multicomponent nature of many fuels contributes to the uncertainties when their data are being compared to the data of pure substances. So while there appears to exist a good workable relation to predict limiting re-

*For a more detailed description of this model see the appendix of Ref. 3.



Burning rate vs. H_c/H_v

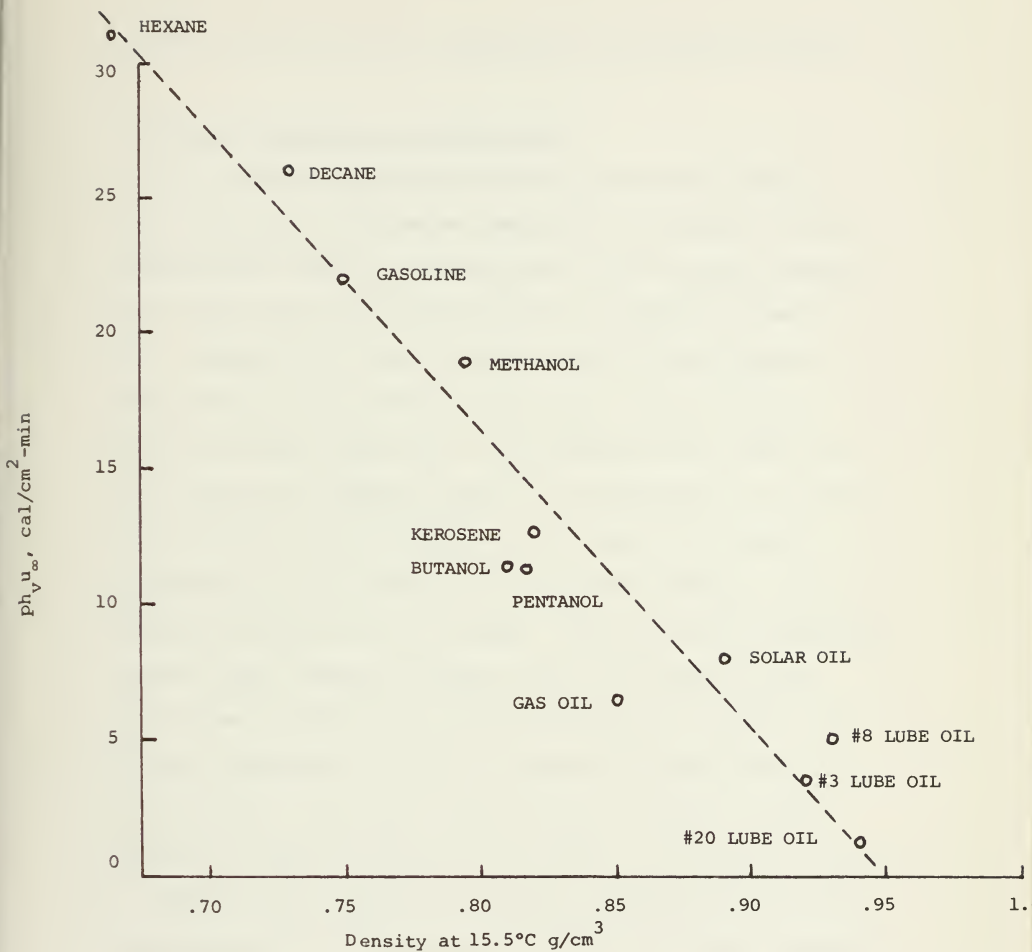
Figure 1-3

gression rates, confirming the accuracy of the linear constant will require additional testing.

Since oils of higher density have, in general, lower regression rates and lower latent heats of vaporization (aromatics are an exception) it was felt there might be some relation between latent vaporization heat and specific gravity. The latent vaporization heat input for a number of oils was plotted against their density, the result appearing here as Figure 1-4. Though several of the data are scattered, a definite band exists inside of which lies the majority of data. If differences in the experiments are taken into consideration, the relation appears valid -- particularly for the higher density oils -- and so may be used to make preliminary estimates as to what the behavior of the heavier fractions might be. The equation for the mid line is

$$\rho u_{\infty} h_v = 110(0.95 - \rho) \frac{\text{cal-cm}}{\text{g-min}} \quad (1-7)$$

Though analytically this indicates that oils with specific gravities greater than 0.95 do not burn there are certainly instances where they do, though not as well as the lighter, more volatile oils. The boiling points of heavy oils are so high ($\sim > 600^{\circ}\text{C}$) that the small amount of heat they receive from a slow free burn cannot compensate for that which is lost to the environment via the large boiling to ambient temperature gradient. Additional information on the burning



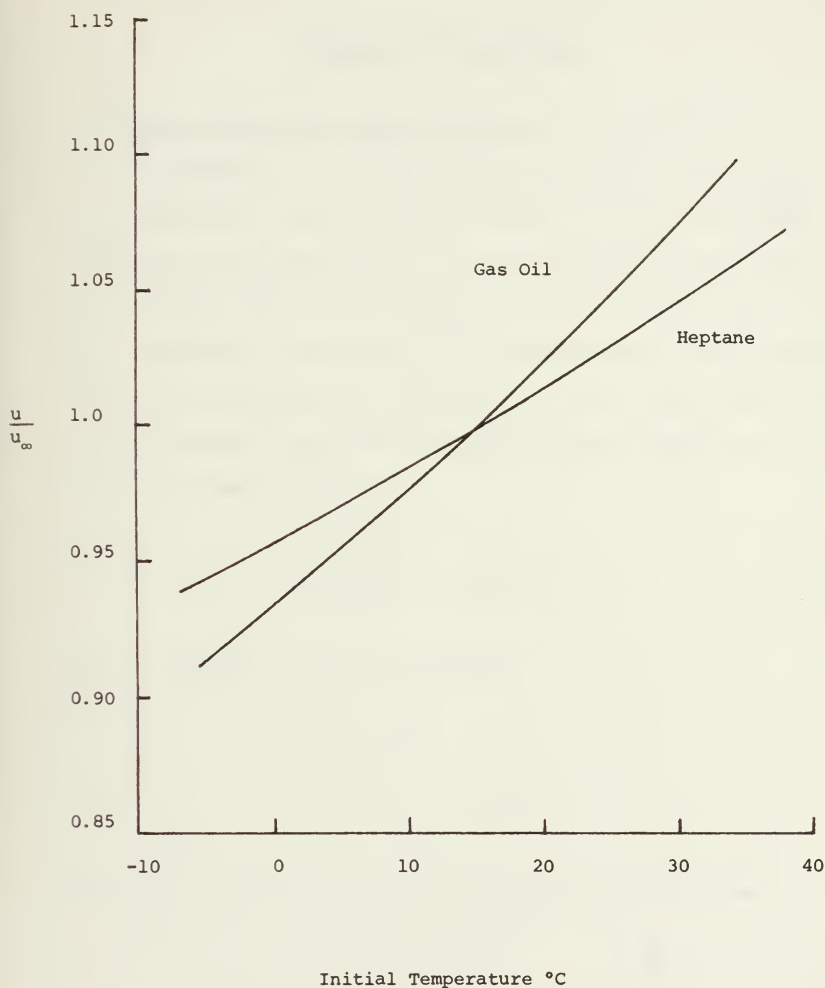
Latent Vaporization Heat Input vs. Fuel Density

Figure 1-4

of heavy oils should serve to substantiate this proposed relation.

3. Effect of temperature on burning rate

All of the data presented so far has been obtained from oil which is initially at an ambient temperature of about 15°C. Before concluding this chapter it should be noted that the ambient temperature of the liquid to some extent affects the limiting regression rate. Certainly, with only a constant amount of heat available, colder oil will burn slower than warmer oil. The more volatile fuels use a smaller proportion of the available heat to preheat the fuel to vaporizing temperature than do the heavier oils. In general, they also have higher specific heats so a change in the initial temperature of the fuel represents a considerable change in the proportion which must be used to preheat. The effect of the temperature change on their limiting regression rates is therefore more pronounced than the effect which would be observed for a heavier fuel. By way of illustration, Figure 1-5 is provided for two fuels, gas oil and heptane. The greater effect is seen in heptane. Overall, however, the change in burning rate is small, on the order of 0.45%/°c. In support of this, Brockis, in reference 16, states that his observations have led him to conclude that the effect of initial temperature is indeed small.



Change in Burning Rate With Ambient Temperature

Figure 1-5

Chapter 2

Temperature Distributions

1. Thermal thickness in unconfined burning

Oil burning with a constant regression rate can be represented as a one dimensional system as shown in Figure 2-1. Here, the surface is imagined to be stationary and the fresh liquid rises to it at the governing regression rate. There is assumed to be an infinite depth of oil. Heat is constantly conducted to the liquid and by the time it reaches the surface its temperature is assumed to be the boiling temperature of the substance. Hence the differential equation describing this system in the steady-state is:

$$\frac{d}{dz} \left(\lambda \frac{dT}{dz} \right) + \rho u c_p \frac{dT}{dz} = 0 \quad (2-1)$$

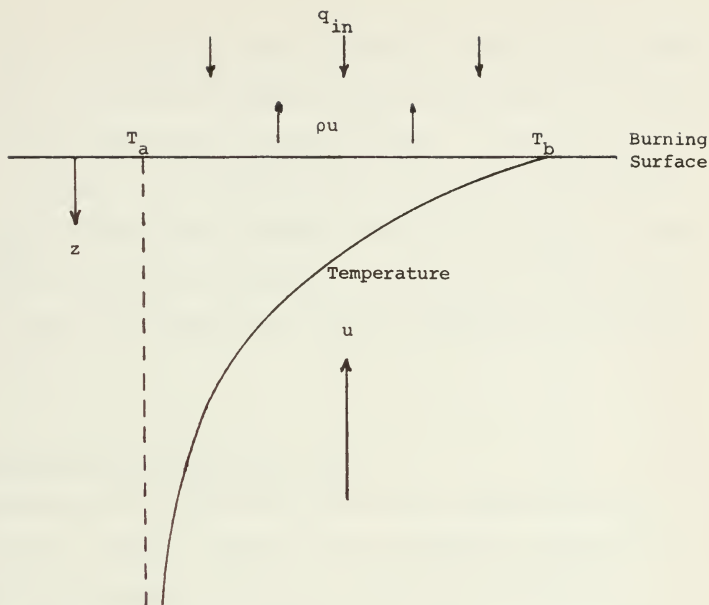
with the boundary conditions as follows:

$$z = 0 \quad T = T_b$$

$$z = \infty \quad T = T_a$$

When q_{in} , ρ , c_p and λ are assumed constant the solution becomes:

$$T - T_a = (T_b - T_a) e^{-\frac{\rho u c_p}{\lambda} z} = (T_b - T_a) e^{-\frac{u}{\alpha} z} \quad (2-2)$$



q_{in} = heat from flames
 mass burning rate

T_a = ambient temperature

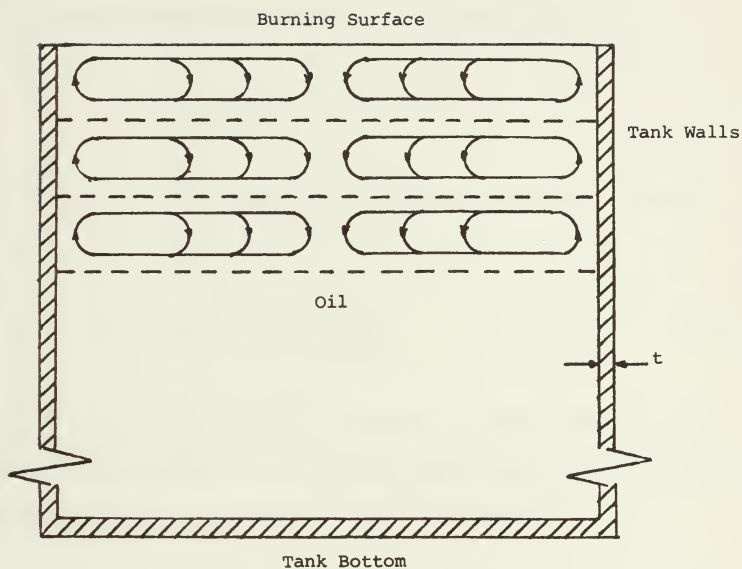
T_b = boiling temperature

Diagram of the Burning Fuel

where $\alpha = \frac{\lambda}{\rho c_p}$, the molecular thermal diffusivity. Due to the relatively low thermal conductivity of most fuels the physical depth over which this distribution takes place is relatively small. In the case of hexane for instance, $u_{\infty} = 0.6$ cm/min and $\alpha = 0.9 \times 10^{-3}$ cm²/sec which makes $\frac{\lambda}{\rho c_p}$, the thermal depth constant, only 0.09 cm. At 3 or 4 thermal thickness the change in temperature is very small so the thickness over which there is any significant change in temperature is on the order of 0.3 cm.

2. Experimental data from fires in tanks.

Experimental data confirm these exponential temperature distributions [4,7,8]. However, because of the requirement to contain the oil which one is burning, variations in temperature profiles are brought about due to the thermal influences of the container used. A great amount of data has been collected by Blinov [4] where he burned oil in tanks of various materials and sizes. When the temperatures are plotted against depth the profiles are indeed exponential but much less steep than would be predicted on the basis of the oil's thermal diffusivity alone. Higher oil temperatures at greater depths are the result of heat conduction through the tank walls. The high conductivity of the wall (most burns were performed in steel tanks) permits a higher than normal temperature to exist below the oil surface. Heat is then transferred at depth to the cooler oil in contact with the wall. Once heated, this oil rises by natural convection and most likely circulates in cells in thin horizontal layers. (see Figure 2-2). Since the plotted



Oil Circulation in Tanks Containing Free Burning Oil

Fig. 2-2

temperature data is exponential, it must be assumed that circulation is limited to thin layers for if it were on a grander scale, there would be a distinctly different profile.

Given the exponential relationship from equation 2-2

$$T - T_a = (T_b - T_a)e^{-kz}, \quad k = \frac{u}{\alpha}$$

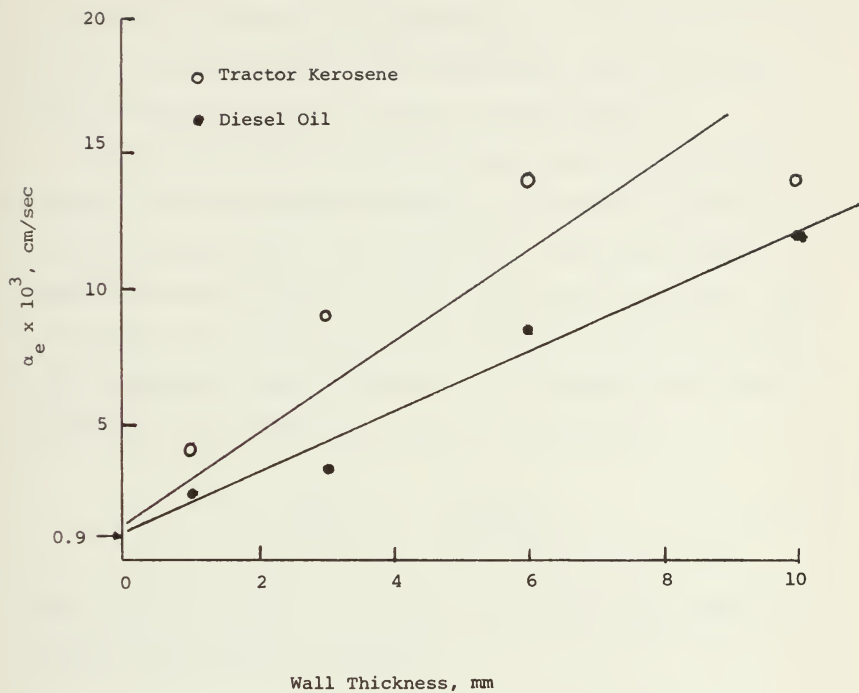
we may determine a new "convective" exponent, k_c from the available data.

$$k_c = -\frac{1}{z} \ln \left[\frac{T - T_a}{T_b - T_a} \right] \quad (2-3)$$

Data shows that for any given tank diameter, k_c varies with tank wall thickness but the regression rate does not [4]. It is then reasonable to define k_c using an "effective" thermal diffusivity.

$$k_c = \frac{u}{\alpha_e} \quad \text{or} \quad \alpha_e = \frac{u}{k_c} \quad (2-4)$$

The effective diffusivity accounts for all the effects of circulation and wall conduction and though the concept lacks a rigorous development, it has attributes which lend credibility to its usefulness. Temperature data taken for a variety of wall thicknesses by Blinov [4] show that k_c decreases (α_e increases) with increases in wall thickness. Plotting the computed values of α_e vs. wall thickness gives a nearly linear relationship. Figure 2-3 shows this for data taken from diesel



Change in effective diffusivity with wall thickness
for circular steel tanks*

Tank diameter = 150 mm

*From data obtained in Reference 4

Figure 2-3

oil and kerosene. Extrapolating the line to zero thickness results in an effective diffusivity of approximately $1.0 \times 10^{-3} \text{ cm}^2/\text{sec}$. This is of course very close to the thermal diffusivity of the pure liquid and what the value for zero wall thickness should be.

If density and specific heat are assumed constant then the differences in the various diffusivities are a consequence of different effective conductivities. We can arrive at a relationship between thermal diffusivity and wall thickness by utilizing this concept. The heat transfer area of the oil is the circular area and that of the tank is the circumference times the thickness. In comparing their relative contributions to the total heat transfer one could write

$$\alpha_e = \frac{\lambda_o}{(\rho c_p)_o} \left[1 + \frac{\lambda_s (\pi d t)}{\lambda_o (\pi d^2 / 4)} \right] \quad (2-5)$$

where o refers to the oil and s refers to the steel. Then, taking the derivative with respect to thickness,

$$\frac{d\alpha_e}{dt} = \alpha_o \left(\frac{4\lambda_s}{d\lambda_o} \right) \quad (2-6)$$

yields a constant slope for any given diameter. Through such an approach we can demonstrate the nature of the linear relationship. Figure 2-3 however, shows slopes of 0.010 and 0.017 cm/sec while substitution of physical values into 2-6 would predict a slope of 0.084 cm/sec-mm. The reason for the great discrepancy lies in the implicit assumption in equation 2-5 of similar temperature gradients in the tank wall and the oil

Heat transfer in the steel is greatly overstated since its temperature gradient is considerably smaller than the oil's. Allowance for this fact would produce a result in 2-6 closer to what is actually observed. Equation 2-6 might more realistically be written as

$$\frac{d\alpha_e}{dt} = \alpha_o \left(\frac{4\lambda_s}{d\lambda_o} \right) \left[\left(\frac{dT}{dz} \right)_s \right] \quad (2-7)$$

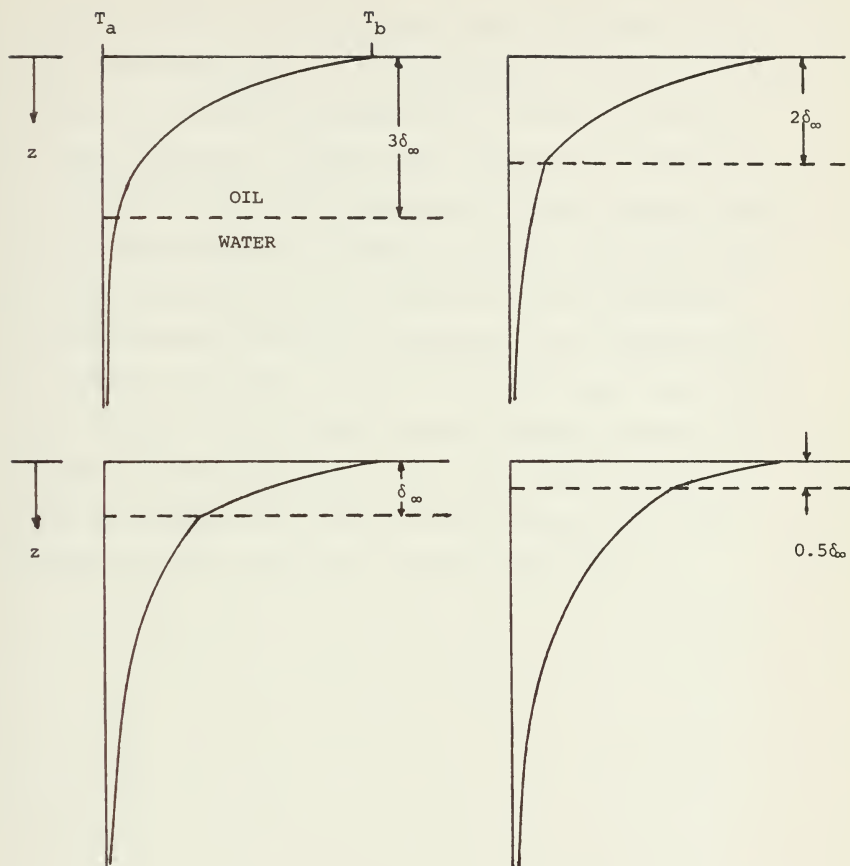
Unfortunately, a distinct lack of wall temperature data in the literature consulted does not permit a direct comparison of this equation with Figure 2-3 to be performed.

3. Finite thicknesses on water.

The previous discussions are all based on having an infinite thickness of oil. When a finite burning layer of oil on top of water is considered, the temperature gradient develops a discontinuity at the interface of water and oil. How great this discontinuity is will depend on the ratio of the thermal conductivities of the two liquids. Water has the greater conductivity and the ratio of its value to that of most oils is about 4.0 to 1. Since the rate of heat transfer across the interface remains constant, the temperature gradient on the water side must be about one quarter as steep as that on the oil side, at that point. This discontinuity is shown graphically in Figure 2-4 which is a series of hypothetical temperature profiles for different thicknesses of oil burning on water.

The change in temperature gradient in the water means that heat will travel to a greater depth before near ambient conditions are reached. The temperature distribution however is still exponential since the interface temperature is increasing in time as the burning oil layer becomes thinner. This entire temperature profile in the water may be approximated in much the same way as the oil's computed profile. That is, the temperature may be considered as a function of $\exp\left(\frac{-u_o}{\alpha_w} z\right)$. total heat capacity of the water is then proportional to its thermal diffusivity.

At 15 °C the diffusivity of water is $1.4 \times 10^{-3} \text{ cm}^2/\text{sec}$ while that of oil is $0.7 \text{ to } 0.9 \times 10^{-3} \text{ cm}^2/\text{sec}$. The ratio of thermal diffusivities therefore ranges between 1.5 and 2.0. At oil thicknesses greater than three thermal thicknesses, the differences in heat transfer between oil and water are minimal since the water sees such a small temperature gradient. As the oil layer is depleted, the differences are more pronounced. The effect of additional heat transfer to the water is evidenced in Figure 2-4 where the area to the left of the water's temperature profile is always greater than a corresponding area on the oil's. Figure 2-4 was drawn for a water-to-oil diffusivity ratio of 2.0. Not only must heat be transferred to heat a proportionately larger volume of water, but must also be provided to meet the demand imposed by the greater specific heat of water. To achieve the same equilibrium temperature distribution in the water then, it must receive between 3 and 4 times as much heat as would be required by the oil for the same distribution. Despite this seemingly large heat demand, the effects on burning rate might at first appear to be small, as explained below.



$$\delta_\infty = \left(\frac{\lambda}{\rho u_\infty c_p} \right)_{\text{OIL}}$$

T_a = AMBIENT TEMPERATURE

T_b = BOILING TEMPERATURE

Temperature Profiles of Burning Oil on Water

$$\text{for } \frac{\alpha_w}{\alpha_o} = 2.0$$

Figure 2-4

For the lighter oil fractions with lower boiling points, the latent heat of vaporization is a high percentage of H_v , the total heat transferred to the oil (see equation 1-5). As such, an increase in the fluid's stored heat, $\int_p c_p \Delta T dz$, due to the presence of water does not significantly detract from the proportion going to vaporize the oil and the burning rate is only slightly diminished. On the other hand, the stored heat portion of H_v for the heavier oils is definitely a significant quantity and one which increases as the temperature profile develops in the water. But due to the much higher boiling point of the heavy oils, the oil-water interface temperature reaches 100 °C at larger oil thicknesses and the rate of heat storage in the water becomes insignificant when compared to the heat which goes to the vaporization of the water at the interface (see chapter 4).

Chapter 3

Effects of Oil Composition on Burning

1. Characteristics of complex oils

Most oils and fuels are complex substances which, unlike pure materials, have a boiling range rather than a specific boiling point. Some part of a complex oil will vaporize at the initial boiling point to be followed by the vaporization of other parts at higher temperatures as the temperature of the oil is raised. The last part of the original mixture will vaporize at the final boiling temperature or end point. Generally the portions evaporated are referred to as fractions in reference to their fractional part of the original substance. A set of typical fractionation curves is shown in Figure 3-1. The average boiling point is sometimes defined as the temperature at which 50% of the fuel has evaporated but more often a mass average boiling point is computed [9]. Such a parameter takes into account the fact that fractions boiled off at the higher temperatures generally have a higher density and molecular weight. The significant fractionation range generally lies between 10% and 90% evaporated so one could also reasonably define an average boiling point to be the average of the temperatures at which those events occur.

$$T_b = \frac{1}{2}[(T_b)_{10\%} + (T_b)_{90\%}] \quad (3-1)$$

Distilled fuels which are fractions of crudes or similar complex oils have small boiling ranges, typically in the neighborhood of 100°C

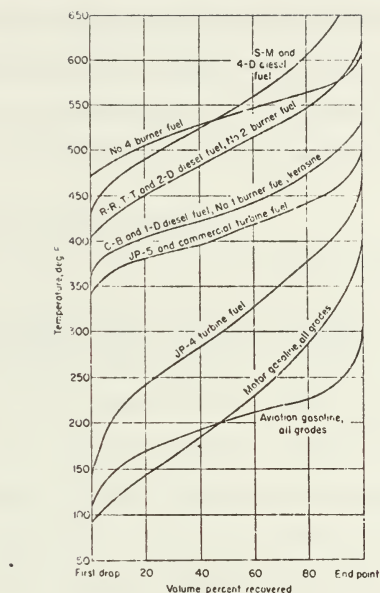


FIG. 2. Typical distillation curves.

A Series of Fractionation Curves

Source: Reference 19

Figure 3-1

or less. The boiling range of a crude oil may extend 400 to 500°C. Since a burning oil layer develops a temperature distribution and may encourage boiling at places other than the surface, it is obvious that boiling and burning of the complex oils cannot be analyzed using the simple model of a pure substance. An approach which recognizes the differences in boiling points and densities must be undertaken.

2. Characteristics of ideal solutions

Solutions of liquids can be classified into three categories [4]:

- (1) Components having unlimited solubility
- (2) Components having limited solubility
- (3) Components that are nearly insoluble

The last category is of no concern to the study of complex oils. The second classification includes mixtures of soluble oils or alcohols and water and has some limited interest but for the most part oils are soluble amongst themselves and must fall under the first category.

Soluble mixtures can be further subdivided into [4]:

- (1) Normal or "ideal" solutions
- (2) Solutions which exhibit a minimum boiling point at some composition
- (3) Solutions which exhibit a maximum boiling point at some composition

It is graphically evident from Figure 3-1 and other sources that petroleum products do not have maximum or minimum boiling points and can therefore be classified as ideal solutions.

Ideal binary solutions are composed of two pure substances, hereafter designated as 1 and 2. The two components are mixed in some proportion and it is the component's mole fraction that is usually used

to describe the makeup of the solution. Such solutions are termed ideal since the components have partial pressures in the vapor phase proportional to their molar fraction in the liquid phase. Thus, if x_1 and x_2 represent respectively, the molar fractions of the first and second component of a liquid binary mixture, their respective partial pressures would be:

$$P_1 = x_1 P_{1,0} \quad (3-2a)$$

$$P_2 = x_2 P_{2,0} \quad (3-2b)$$

where $P_{1,0}$ and $P_{2,0}$ are the partial pressures of the pure component at temperature T_0 .

The most basic law concerning ideal mixtures is that the vapor of such a mixture is richer than its liquid in the component that has the higher vapor pressure. The molar makeup of the vapor is then always different from the liquid. With reference to the laws governing ideal gases, the molar fraction of one gaseous component is the ratio of its partial pressure to the total pressure. Thus,

$$y_1 = \frac{P_1}{P_1 + P_2} \quad (3-3a)$$

$$y_2 = \frac{P_2}{P_1 + P_2} \quad (3-3b)$$

where y_1 and y_2 are the molar fractions of the first and second component that are present in the vapor phase. For a constant pressure system,

e.g. - atmospheric pressure, the following relations can be developed.

$$P_0 = P_1 + P_2 = x_1 P_{1,2} + x_2 P_{2,0} = \text{constant}$$

but since

$$x_1 + x_2 = 1$$

$$P_0 = P_{1,0} + x_2 (P_{2,0} - P_{1,0}) \quad (3-4)$$

and

$$x_2 = \frac{P_{1,0} - P_0}{P_{1,0} - P_{2,0}} \quad (3-5)$$

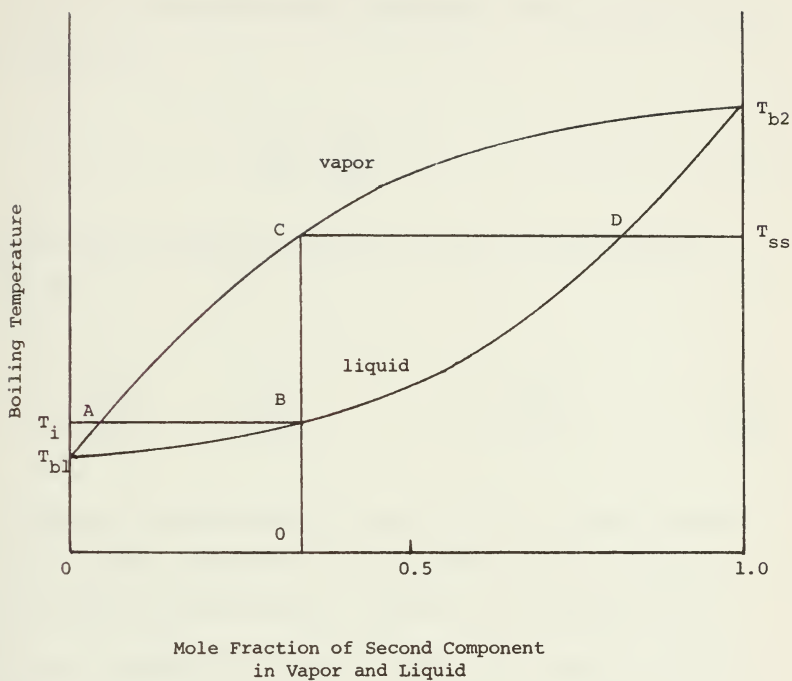
Substitution of 3-2 into 3-3b results in:

$$y_2 = \frac{x_2 P_{2,0}}{P_{1,0} + x_2 (P_{2,0} - P_{1,0})}$$

or

$$y_2 = \frac{\frac{P_{2,0}}{P_{1,0}} x_2}{1 + \left(\frac{P_{2,0}}{P_{1,0}} - 1 \right) x_2} \quad (3-6)$$

Equation 3-6 shows the clear relation between gaseous and liquid fractions. In such a constant pressure system this relationship changes with temperature since both $P_{1,0}$ and $P_{2,0}$ increase at different rates with increases in temperature. When P_0 is atmospheric pressure the solution is boiling. Then by allowing the subscript 2 to represent the component with the higher boiling point a plot of the molar fraction in the vapor and liquid against boiling temperature results in the curves displayed in Figure 3-2.



Typical Boiling Temperature - Composition Curve
for an Ideal Binary Solution

Figure 3-2

The precise determination of these curves may be found by referring to the Clausius-Clapeyron relationship between vapor pressure and temperature.

$$\frac{1}{p} \frac{dp}{dT} = \frac{h_v M}{RT^2} \quad (3-7)$$

Applying this to equations 3-5 and 3-6 results in the following functions

$$T = T(x_2) \quad (3-8a) \quad x_2 = x_2(T) \quad (3-8c)$$

$$T = T(y_2) \quad (3-8b) \quad y_2 = y_2(T) \quad (3-8d)$$

The details of the development of these functions is given in Appendix A. The only data needed to use the relations is the atmospheric boiling point of each component. One may use the average value of $\frac{h_v M}{RT_b}$ given in Appendix A or compute a more precise constant according to the procedure listed there.

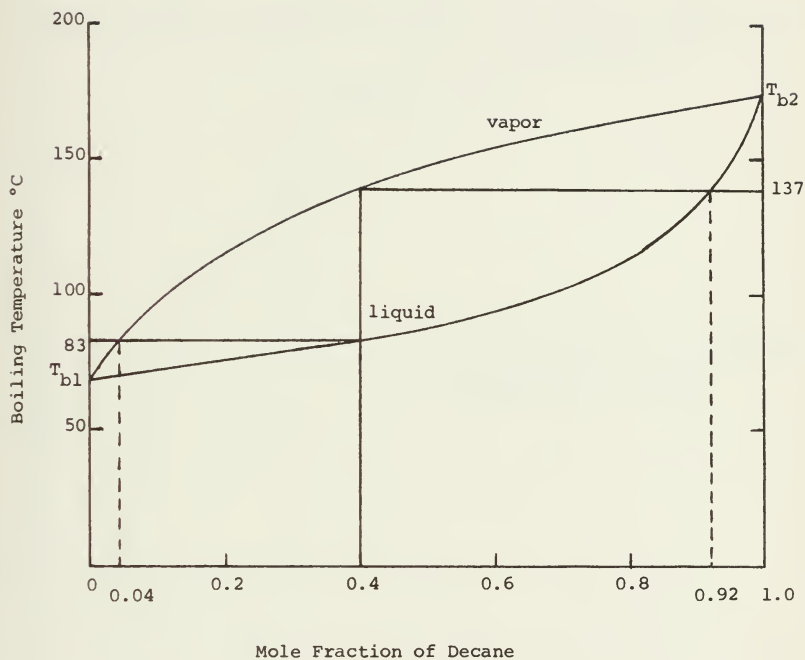
These boiling temperature-composition curves are directly applicable to the burning problem and information contained therein can be most useful. At 0% and 100% concentrations of the heavy component, the boiling point of the liquid is merely that of the pure component, 1 or 2, respectively. At any temperature in between, the vapor has a second component concentration different from the liquid and always smaller. If, in Figure 3-2, burning were to be taking place at T_1 , the initial boiling temperature, the vapor would have

the composition of point A. The lighter substance (component 1) would then be depleted at a rate faster than it could be supplied from the liquid and the makeup of the ambient liquid must shift to the right. Now unless the two components have markedly different densities or other such peculiarity, there is no documented evidence that the concentration of the ambient liquid changes at all. In order to retain the original proportions in the unheated liquid the burning vapor must have the same composition as the liquid, represented by the vertical line BC. The temperature at which $y_2 = x_{2,0}$ the original mole fraction of the heavy component in the liquid solution is T_{ss} , the steady state boiling temperature. The composition of the surface layer of liquid oil at that temperature is defined by point D. It is obvious then that in addition to a temperature gradient there must also exist a concentration gradient in the top layers of a burning binary solution. The equilibrium concentration profile reflects the liquid composition at each temperature along the temperature distribution curve (Figure 2-1) as defined by equation 3-8c.* This concentration profile is not purely exponential like the temperature distribution since $x_2(T)$ is not linear. Furthermore, the composition is the same as the original composition at all temperatures below T_1 , the initial boiling temperature. Indeed, this thickness over which composition changes is so shallow that the equilibrium concentration profile is nearly linear.

*It will be necessary either for the light component to diffuse through the liquid to the surface (a very slow process) or to vaporize below the surface and escape to provide the equivalent in gradient that the equilibrium model used here requires (see Section 5).

As an example of all these relationships, Figures 3-3 and 3-4 display the results which are predicted for a mixture of 60% hexane and 40% decane. The initial boiling temperature is 83°C while the steady-state surface temperature is 137°C. It should be noted that the equilibrium composition remains unaltered below 0.056 cm, which is less than even one thermal thickness on the temperature profile. The sharp discontinuity in the concentration profile at this point is unrealistic in nature and more than likely there exists sufficient diffusion that tends to smooth the profile to a more reasonable shape as indicated by the dotted line. Even so, the changes in composition remain sharp in the uppermost layer.

Not surprisingly, there have been no experimental results reported which would tend to support or deny the existence of this model. To accurately take samples in free burning oil mixtures at depths of less than 1 mm below a regressing surface is just about an impossible task. Where work of this nature has been accomplished has been in tanks and small burners where, as was pointed out earlier, the temperature profile extends much deeper due to additional heat conduction in the wall. Along with the extended temperature profile one would also expect to see an extended equilibrium composition profile making it possible to take samples at more realistic depths. Blinov [4] gives some data for ideal solutions of alcohols which were taken from small burners of 29.5 mm diameter. This data for mixtures of ethanol and butanol and ethanol and isoamyl alcohol is presented here in graphical form as Figures 3-5 and 3-6. There was no temperature distribution

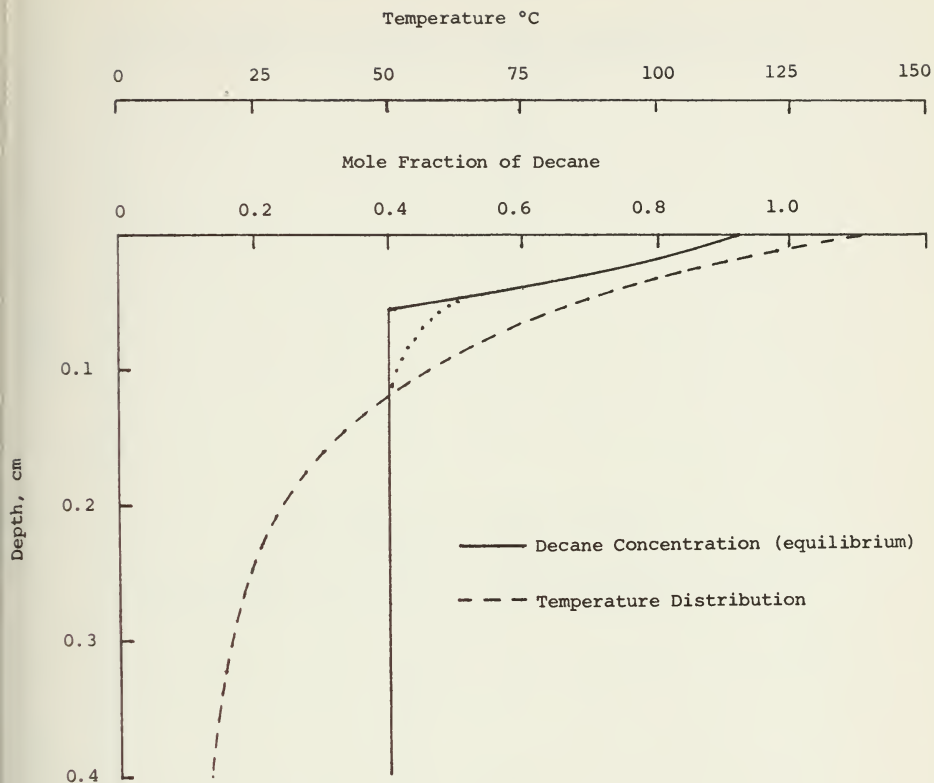


$$T_{b1} = 68.7^{\circ}\text{C}$$

$$T_{b2} = 174^{\circ}\text{C}$$

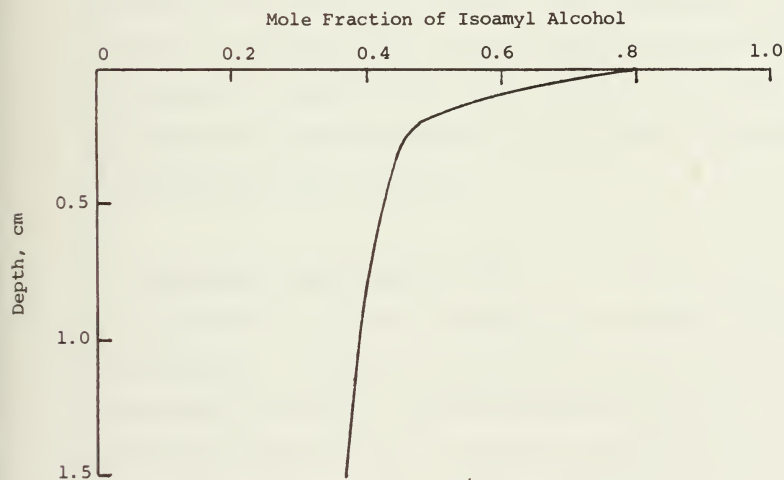
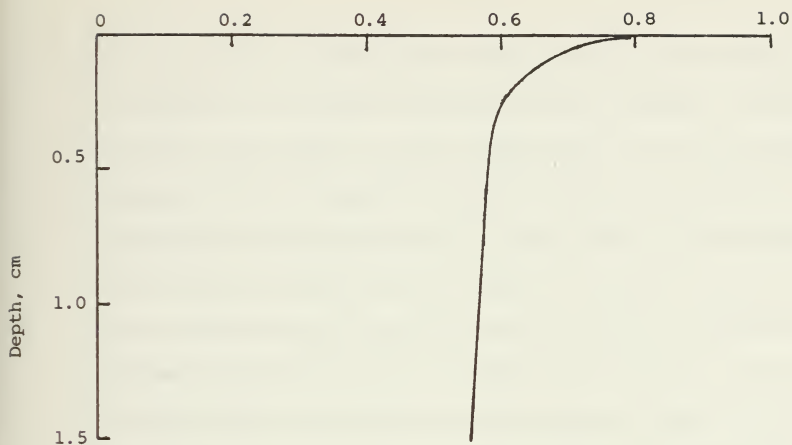
Boiling Temperature - Composition Curve for a Solution
of 60% Hexane and 40% Decane

Figure 3-3



Equilibrium Concentration Profile for Decane
in a Burning Solution of 60% Hexane - 40% Decane

Figure 3-4



Concentration Data from Burning Mixtures of Alcohols*

Figure 3-5 (top) - 45% Ethanol - 55% Butanol

Figure 3-6 (bottom) - 67% Ethanol - 33% Isamyl Alcohol

*Source of data is Reference 4.

data given but it is certain that the distribution was extended as a consequence of the burner walls and the small diameter. Samples of the mixture were taken at various depths below the burning surface and analyzed for their composition. What is immediately apparent in the plotted data is the resemblance of a sharp change in concentration gradient a short distance below the surface. The close resemblance of this to that which was predicted analytically for the hexane-decane combination lends some degree of support for the model. It is still uncertain whether the compositions represented in Figures 3-5 and 3-6 are in fact the equilibrium compositions and just how much diffusion has taken place to alter their profile. Only a knowledge of the temperature distribution can provide the required information that would permit the comparison to be made. These are not available and the theories for such distributions in small burners are inadequate to even predict them analytically.

3. Application of model to real oils

As pointed out earlier, a complex oil is actually a mixture of many substances. An accurate characterization of an oil would entail identifying the dozens of individual components and their fractional parts of the whole solution. To carry out a detailed analysis of the burning of such a substance in the manner developed above would be extremely difficult and of questionable benefit. A more practical approach is to treat the oil as a binary substance consisting of a light and a heavy fraction. What these fractions should represent

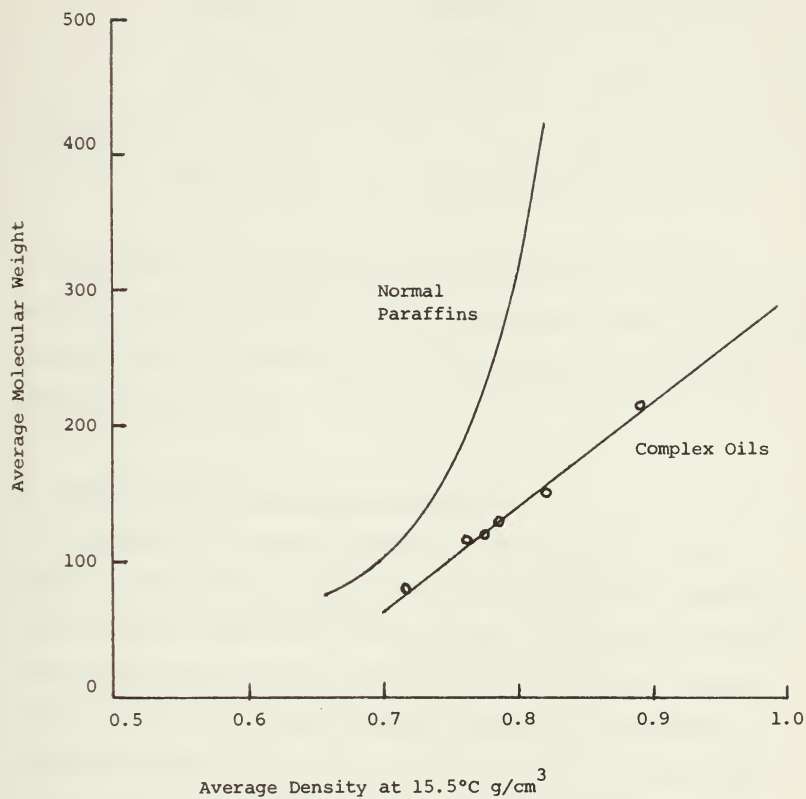
is open to debate but a reasonable approximation may be obtained by referring to some fractionation data. It is proposed to let the light fraction be represented by the oil that is distilled at the 10% level and the heavy fraction by that at the 90% level. By and large, most distillation curves are linear in this region so a proper apportionment of each fraction would be about 50% by volume. The model developed for the burning of binary solutions, however, is based on mole fraction, not volume fraction. Conversion to mole fraction may be approximated by the following equation, this for the first component.

$$(MF)_1 = (VF)_1 \left(\frac{\rho}{M} \right)_1 \times \frac{1}{2} \left[\left(\frac{M}{\rho} \right)_1 + \left(\frac{M}{\rho} \right)_2 \right] \quad (3-9)$$

Here, MF is the mole fraction, M is molecular weight and VF is the volume fraction. While the volume fraction can be estimated from the distillation curves, molecular weight must be determined by other means. A compilation of data from several sources [9 through 12] has resulted in the graph shown in Figure 3-7. For complex oils there is a linear relation of molecular weight to density. From this one may obtain the values necessary to use equation 3-9. The mole fraction for the heavier fraction may be computed similarly or one may use

$$(MF)_2 = 1 - (MF)_1$$

For the hexane-decane example above, the mole fractions may be computed using the following given information:



Molecular Weights vs. Density for Typical Fuels

Figure 3-7

Hexane (1)

M = 86
 $\rho = 0.6637$
 VF = 0.5

Decane (2)

M = 142
 $\rho = 0.7333$
 VF = 0.5

Then using 3-9,

$$(MF) = 0.62$$

$$(MF)_2 = 0.41$$

As stated above, these fractions are only approximate due to the averaging assumption of $\frac{M}{\rho}$ in 3-9. What the results show is that the mole fractions of 0.6 for hexane and 0.4 for decane may be used without being too much in error.

4. Density differences present in burning

According to the theory developed for the burning of binary substances the surface of the oil is richer in the heavier component than the layers immediately below the surface. The question naturally arises, does this difference in density create an unstable situation which would cause the surface material to sink and be replaced by a layer with a higher proportion of light component? If such a situation did exist, it is easy to see why the vapor contains light fractions in higher proportions than the surface from which they were vaporized. Basically, a balance must be made between the gain in density at the surface due to the loss of lighter more volatile fractions and the loss in density due to the higher surface temperature. Letting the subscripts o and s represent the original and surface conditions

we can write:

$$\Delta\rho = \rho_o = \rho_s = (\rho_1)_o + x_{2,o}\Delta\rho_o - [(\rho_1)_s + x_{2,s}\Delta\rho_s] \quad (3-11)$$

where

$$\Delta\rho_o = (\rho_2)_o - (\rho_1)_o \quad (3-12a)$$

$$\Delta\rho_s = (\rho_2)_s - (\rho_1)_s \quad (3-12b)$$

and $x_{2,o}$ and $x_{2,s}$ are mass fractions of the second component. The densities at the surface may be defined as:

$$(\rho_1)_s = (\rho_1)_o (1 - \beta_1 \Delta T) \quad (3-13a)$$

$$(\rho_2)_s = (\rho_2)_o (1 - \beta_2 \Delta T) \quad (3-13b)$$

where $\beta = -\frac{1}{\rho} \frac{d\rho}{dT}$, the volume expansion coefficient and $\Delta T = T_s - T_i$.

By assuming $\rho_1 \approx \rho_2 \approx \rho_o$, and dividing 3-11 by ρ_o (after substituting 3-13) we arrive at

$$\frac{\Delta\rho}{\rho_o} = \frac{\Delta\rho_o}{\rho_o} (x_{2,o} - x_{2,s}) + [\beta_1(1-x_{2,s}) + \beta_2 x_{2,s}] \Delta T \quad (3-14)$$

Now since $x_{2,s} > x_{2,o}$, the first term is always negative whereas the second term is always positive and since $\beta_1 \approx \beta_2$ may be approximated as $\beta \Delta T$. When $\frac{\Delta\rho}{\rho_o}$ is negative, the layers are unstable and must sink. Positive $\frac{\Delta\rho}{\rho_o}$ indicates a stable system. Utilizing the results of the

hexane-decane mixture will provide an example of this. If mole fraction can be approximated by mass fraction then,

$$\begin{array}{lcl} x_{2,o} = 0.40 & & \\ x_{2,s} = 0.91 & \text{at } 83^{\circ}\text{C} & \left\{ \begin{array}{l} \Delta\rho_o = 0.0638 \text{ g/cm}^3 \\ (\rho_o)_{\text{avg}} = 0.640 \text{ g/cm}^3 \\ \beta = 0.00125 /^{\circ}\text{C} \end{array} \right. \\ \Delta T = T_{ss} - T_i = 54^{\circ}\text{C} & & \end{array}$$

$$\frac{\Delta\rho}{\rho_o} = (0.0508) + (0.0675) = +0.0167$$

The positive result indicates the surface layer is indeed stable. Numerous calculations with other substances also show a positive value. The stability exists because larger differences in density are accompanied by correspondingly large differences in temperature. In general, the denser the component the higher is its boiling point. Figure 3-8 shows this relationship for several oil families.

It is possible however that the denser fractions are denser at their higher boiling temperatures than the lighter fractions are at their lower boiling temperatures, a situation which might cause turnover of the surface. Figure 3-9 shows what the actual densities of these substances are at their boiling points and demonstrates that this is not the case; if anything, quite the reverse is true. Thus it can safely be concluded that the surface layer remains as originally proposed by the binary burning model. There is no turnover due to density differences since the decrease in density caused by the higher surface temperature provides the stability that is observed.

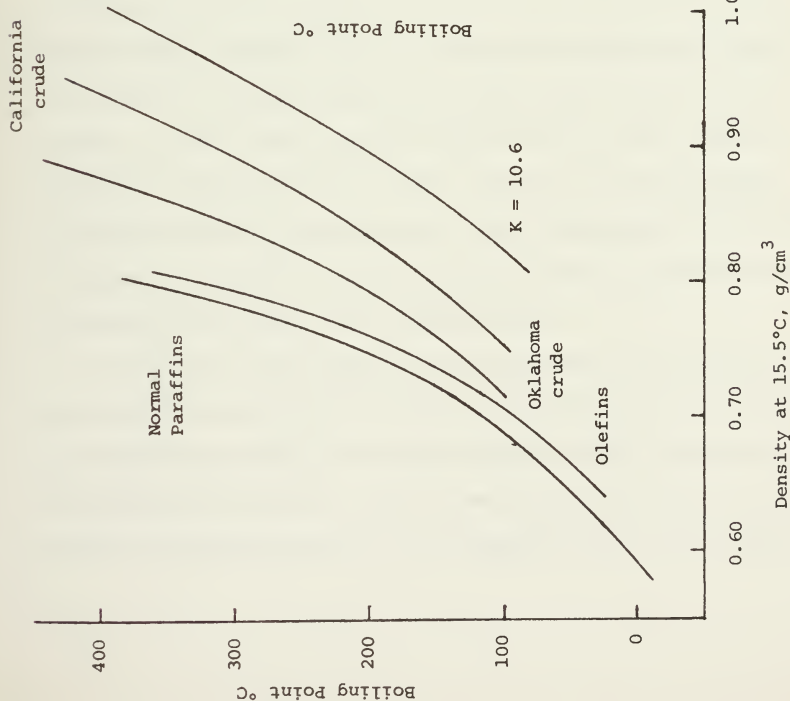


Figure 3-8

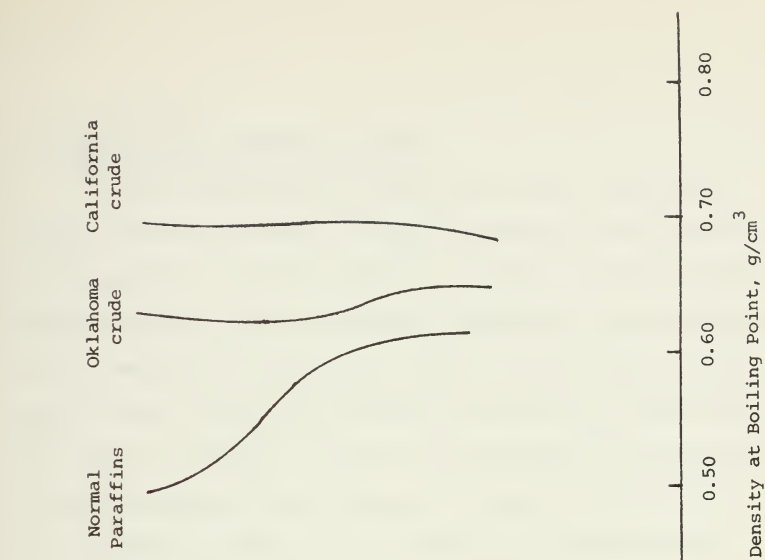


Figure 3-9

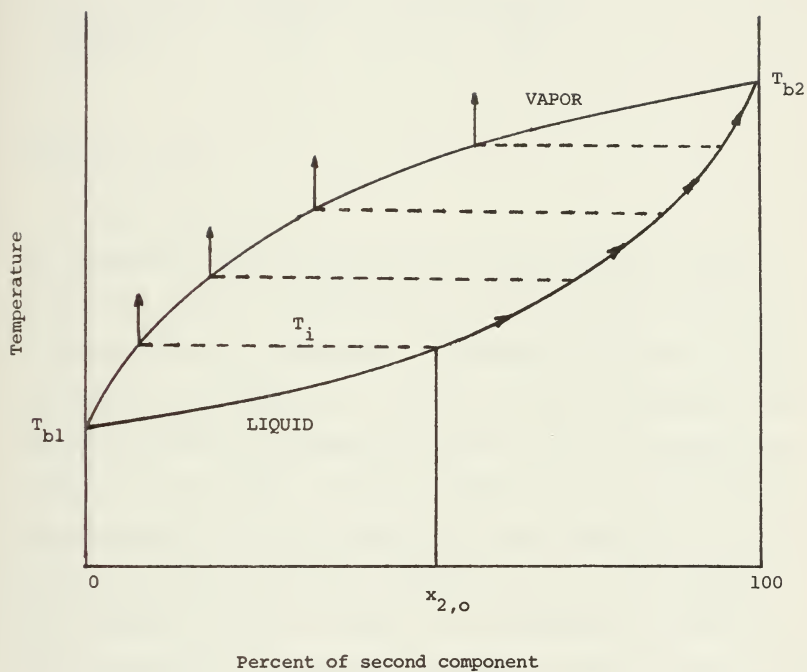
5. Depth at which vaporization begins

In steady state burning the vapor has a higher percentage of lighter component than does the liquid surface where the vaporization is taking place. For this situation to persist the lighter component must be vaporizing below the surface, bubbling up to the surface and then becoming part of the surface vapor. For vaporization to take place at depth there must be nucleation sites or such bubble formation would be explosive. It must also be realized that vaporization of the light component must necessarily involve mass diffusion of that component through the liquid solution and into the growing bubble. Such processes are slow so it is not expected that any vapor bubble being formed will achieve any great size before it rises the very short distance (~ 1 mm) to the surface to join the burning vapor. Though there is no conclusive evidence that nucleation sites exist it shall be assumed, with good reason, that they are present. In oils other than the purest there is a great amount of suspended microscopic foreign matter. Any one of these particles could be a potential nucleation site. Thus vaporization of the lighter component, or some combination of it and the heavy, occurring at some depth below the surface is not inconceivable.

For vapor to form beneath the surface some amount of vaporization heat has to be transferred away from the surface and to that location. The temperature profiles previously computed assumed that only the heat required to raise the liquid's heat capacity was being transferred because the liquid received all its vaporizing heat at the surface.

With more heat passing through the thermal layer the temperature profile is extended so that boiling of the lighter component is initiated at some depth below what the theoretical temperature distribution would predict. The final exiting vapor must have the composition of the original mixture. Since the surface is richer in the heavier component the vapor which is formed below the surface must be richer in the light component. To determine just where this initial vaporization takes place requires analysis of the following model.

Consider a given mass of oil well below the surface. This mass is rising to the surface at the governing mass burning rate. As it reaches a zone where the temperature is high enough to start evaporating the more volatile component its mass velocity is reduced. Rising further, additional amounts of vapor are generated, these containing more of the heavy component. The mass velocity must go to zero at the surface while the final quantity to be vaporized is imagined to consist entirely of heavy component. Essentially then, this original mass of oil has traveled along the liquid line of Figure 3-10, starting at some temperature T and finishing at T_{b2} . At each location it has generated vapor that has a composition determined by the vapor line at that temperature. At the beginning the vapor is richer in the first component than the liquid's composition but by the end it is generating more second component vapor. A summation of all the vapor generated will be a vapor that has the same composition as the original liquid.



Movement of Liquid and Vapor during Vaporization

Figure 3-10

The details of this analysis are presented in Appendix B. The solution for the depth of a layer which begins vaporization at temperature T is:

$$z = \frac{2\lambda}{\rho u_1 \sqrt{Q}} \left[\tanh^{-1} \frac{2aT_{b2} + b}{\sqrt{Q}} - \tanh^{-1} \frac{2aT + b}{\sqrt{Q}} \right] \quad (3-14)$$

where $T = T - T_{b1}$

$$T_{b2} = T_{b2} - T_{b1}$$

The properties of the two components had to be averaged to arrive at this result. Further, the functions $x_2(T)$ and $y_2(T)$ were linearized in the region of T_{b2} to facilitate the taking of derivatives for final integration. Definitions of a , b and Q are found in Appendix B. What procedure to follow to determine the correct initial vaporizing temperature, T , is not clear. It must be chosen such that the integrated vapor evolved from T to T_{b2} will be the proper composition. The temperature at which x_2 equals the original fraction of heavy component is a realistic value for the vapor at that temperature is very rich in the light component. If one were to compute an upper bound for the depth T_{b1} could be chosen instead though there is usually little difference between the two (see Figure 3-3). When these substitutions are made for the hexane-decane example the computed depth is 0.080 cm. As was previously hypothesized, this depth is deeper than what the theoretical temperature distributions would predict. That depth is 0.056 cm. The 40% increase in the depth of the layer over which vaporization occurs

is attributed primarily to the increased demand for heat at that depth.

CHAPTER 4

Effects of the Water Sublayer

1. Oil thicknesses from spills

Before attempting to analyze burning oil that is floating on a water surface it would be worthwhile to review the work previously accomplished concerning the behavior of oil on water. This has been an area of extensive investigation and has resulted in significant contributions by Blokker [13], Fay [14,15] Berridge [16] and others [17]. The theories and research address the problems of oil spreading, oil evaporation and changing properties of the oil. The oil spreading problem is perhaps the most significant since it happens first while the other effects take place over longer periods of time. The thicknesses of the oil layers both during and after spreading have important effects on the burning and heat transfer that will occur.

There are basically three regimes which affect a spreading oil. The initial phase is inertial in which a quantity of oil in a small area will begin to spread due to the predominance of gravitational forces on the initial thickness. As the outer edges of the oil move away and the thickness is reduced, the counteracting viscous forces in the oil and between the oil and water play a larger role in this second phase. As the oil adopts a more uniform thickness and gravitational and viscous forces become negligible, the forces arising from surface tension ultimately control the final spreading phase. The first and second phases take place over relatively short periods

of time, on the order of a few minutes for a given quantity of oil [13], and are of limited usefulness for determining the ultimate size of an oil pool that is to be burned. Limiting pool diameters and thicknesses are then both a function of time and the nature of the surface tension forces. Blokker [13] has developed an empirical relationship between pool radius and time which has been supported by experiment. This expression is

$$\frac{\pi(r_t^3 - r_i^3)\rho_w}{3v(\rho_w - \rho_o)\rho_o} = K_r t \quad (4-1)$$

and is good for initial spreading up until the time when thicknesses are more a function of surface tension. Subscripts w and o represent water and oil respectively, r_t is the radius at time t and r_i is some initial radius, usually negligible. The volume of oil is v while K_r is a constant that depends on the characteristics of the oil in question. Berridge [16] has determined some constants for several crude oils which are presented here in Table 4-1. Replacing r by $\frac{v}{\pi\delta}$ the average thickness, δ , may be computed as

$$\delta = \frac{k}{t^{2/3}} \quad (4-2)$$

where

$$k = \left[\frac{v}{t} \right]^{1/3} \left[\frac{\rho_w}{3\rho_o(\rho_w - \rho_o)K_r} \right]^{2/3}$$

Table 4-1

Crude Oil	$K_r \frac{\text{cm}^3}{\text{g-sec}}$
Libyan	1085
Iranian Heavy	750
Kuwait	1480
Iraq	975
Venezuela	1340

The equilibrium thickness for a spreading oil is the result of a balance of the surface tension forces and was originally presented by Langmuir [18].

$$\delta_{eq} = \left[\frac{-2(\sigma_w - \sigma_o - \sigma_{wo})\rho_w}{g\rho_o(\rho_w - \rho_o)} \right]^{\frac{1}{2}} \quad (4-3)$$

The summation of the water, oil and water-oil interface surface tension, σ_w , σ_o , and σ_{wo} is commonly termed the spreading coefficient, F_s .

$$F_s = \sigma_w - \sigma_o - \sigma_{wo} \quad (4-4)$$

Oil will spread to a theoretically zero thickness when F_s is positive but will adopt a finite thickness when it is negative. By combining equations 4-2 and 4-3 it is possible to estimate the time required to achieve the equilibrium thickness. Assuming $F_s < 0$,

$$t_{eq} = \frac{0.56}{K_r} \left[\left(\frac{v}{\pi} \right)^2 \left(\frac{g}{-F_s} \right)^3 \left(\frac{\rho_w}{\rho_o(\rho_w - \rho_o)} \right) \right]^{\frac{1}{4}} \quad (4-5)$$

For a volume of 100 m^3 of Iraq crude oil (83 tons) this time is approximately 16 minutes if $F_s = -1.0 \text{ dyne/cm}$. The equilibrium thickness would be 0.120 cm.

Direct substitution of real values for surface tension into equation 4-4 shows that a great many oils have positive spreading coefficients. Other effects, however, tend to modify the effects brought about by surface tension alone and result in an effective reduction in the value of F_s . These effects include the limited solubility of the oil in water, evaporation of the oil and eventual emulsification of the remaining oil.

Solubility effects have been recognized by Hillstrom with the example of benzene [18]. At 20°C its computed spreading coefficient is +8.8 but when spilled on water it forms a stable pool with some constant radius indicating a negative F_s . The spreading coefficient became negative as a result of the loss in surface tension of the water which was caused by the partial dissolving of benzene into the water at the interface. Other hydrocarbons have similar limited solubilities which likewise reduce σ_w . Besides the oil itself, certain other ingredients have been shown to have a great influence on the surface tension of water and the spreading of oil. Blokker reports that water with an initial surface tension of 72.8 dyne/cm when treated with sodium alkyl sulfate has a reduced surface tension of 52 dyne/cm [13].

The water, however, need not necessarily be precontaminated to effect a change in surface tension. Soluble surface-active agents that might be carried by the spreading oil itself might dissolve and change the properties of the interface sufficiently to bring about a layer negative spreading coefficient.

Both evaporation of the more volatile fractions of an oil and the thickening which results from its combination with water make an oil more viscous and more resistant to spreading. References 13, 16 and 17 have reported on these effects but there is no universal model available with which one could make accurate quantitative predictions of their effect on final thicknesses. Results from the experiments indicate that effective evaporation or emulsification can take place anywhere from 3 to 30 hours after an oil is first exposed to the water environment. At least one investigator [16] sees these effects as having greater importance than the surface tension balance. This may be true but since the time frame for the occurrence of these events is large their effect on final oil thickness can be important only in instances where the quantity of oil is very large. A more thorough analysis of the effects of weathering an oil thickness might very well be useful but such an analysis cannot be attempted here. For the present, only the surface tension effects will be considered in greater detail.

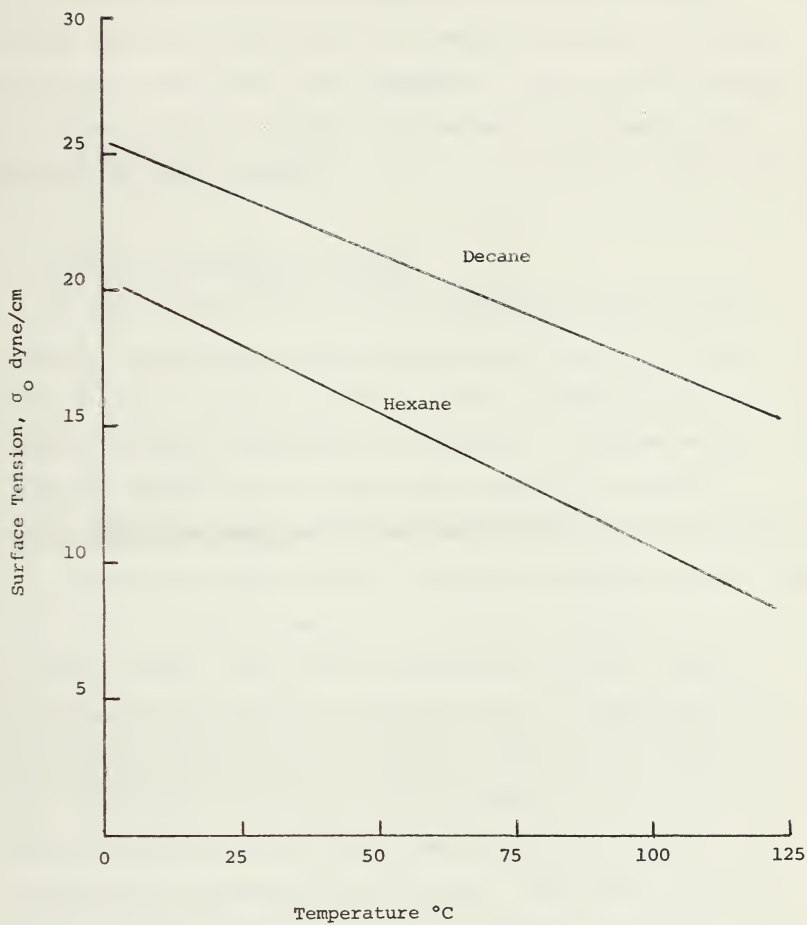
By knowing the volume of the spilled oil and measuring its equilibrium radius, Hillstrom was able to compute thicknesses and spreading coefficients for three hydrocarbons [18].

	$\underline{F_s}$	$\underline{h_{eq}}$
Decane	-2.4	0.140 cm
Decalin	-8.0	0.270 cm
Hexadecane	-9.0	0.300 cm

In the normal paraffin family, isopentane, hexane and heptane have spreading coefficients of +9.4, +3.4 and +0.4 respectively. Decane and hexadecane are listed above. There is a clear trend in this family of hydrocarbons toward lower spreading coefficients with increasing molecular weights. This may be true in the general sense too, but additional experimentation is required to verify the trend.

Surface tension is also greatly affected by temperature. Figure 4-1 shows this relationship for hexane and decane [18]. An oil may have a negative F_s at 20°C but when it is burning the layer has a temperature high enough to reduce σ_o to a point where F_s becomes positive. At this point the fuel lens is no longer in equilibrium and will commence to spread. In decane, for example, $\sigma_o = 22.9$ dyne/cm at 20°C. F_s will go to zero when σ_o falls to 20.5 dyne/cm; this occurs at 60°C. Since the boiling point of decane is 174°C the average temperature of the burning layer will be greater than 60°C and spreading will occur as it tries to burn. The resulting thinner thickness may have some deleterious effects on the fuel's ability to continue burning.

One additional method of affecting the spreading coefficient of an oil might be to add chemicals which themselves have a large negative



Surface Tension as a Function of Temperature

Figure 4-1

F_s . Hillstrom attempted this by adding to a layer of hexane some ethylene iodide ($F_s = -26.5$) [18]. The expected thickening of the oil layer did not take place in this experiment. There is little additional evidence available to support this hypothesis so it cannot be regarded as an effective method.

2. Influence of the water on burning

Consider now that an oil layer has established itself on water according to the spreading mechanism just covered, has been ignited, and is burning. The water beneath now plays an important role in affecting the total heat transfer of the system. Its effect on the temperature distribution has already been introduced in Chapter 2. What is desired are some quantitative results of the water's influence.

Figure 2-4 was drawn for oils in general by assuming a constant heat input, which is a good assumption, and a constant regression rate which of course is false. Heat which was previously available to vaporize the oil must now be diverted to heat the water. The subsequent slower rate of oil vaporization must necessarily result in a lower regression rate. Heat content of the water may be estimated by considering the water-oil thermal diffusivity ratio, the specific heat of water, and the temperature difference across the water. This latter quantity is in part determined by the regression rate (equation 2-2), which is also a function of the water's heat capacity. In performing a quasi-steady analysis we can look at the oil and water at different times (oil thicknesses) and determine the regression rate at that moment. The

constant heat input, q_s , is obtained from

$$q_s = \rho u_{\infty} H_v \quad (4-6)$$

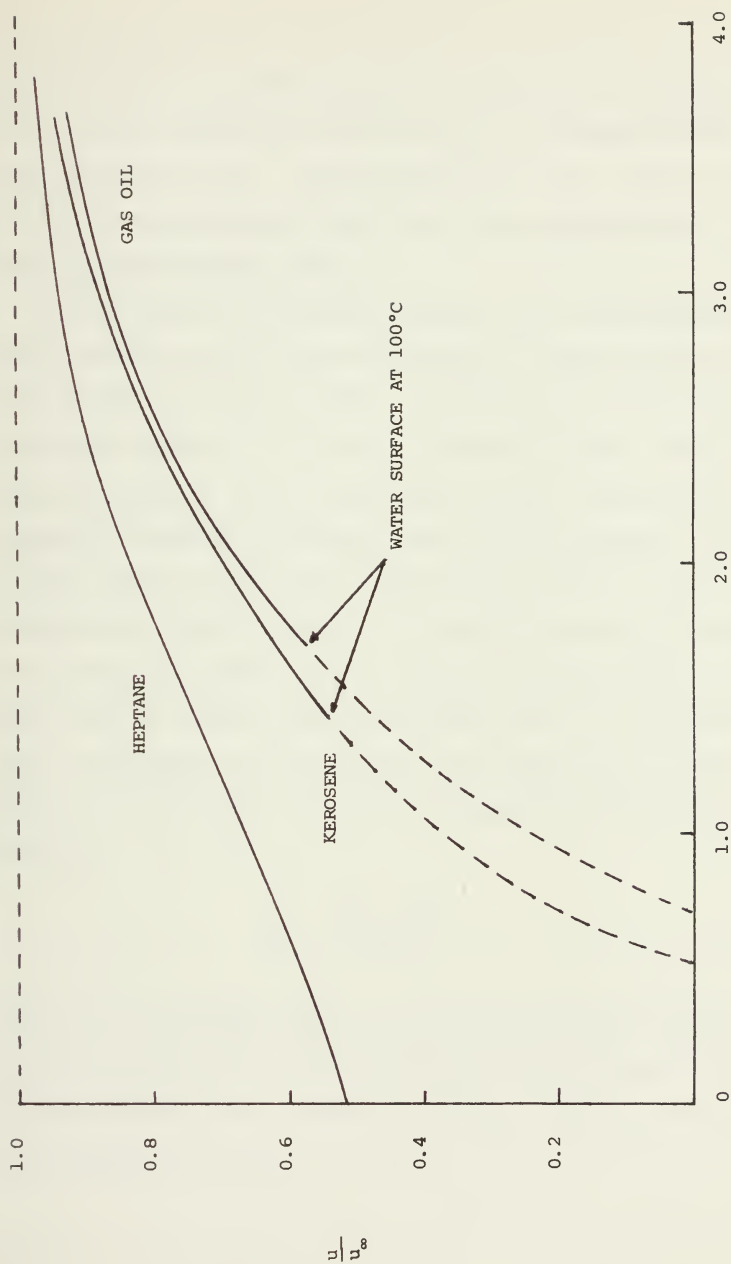
The expression for heat input to the water and oil is:

$$q_s = \rho u [h_v + c_{po} (T_{bo} - T_i) + \frac{\alpha_w}{\alpha_o} C_{pw} (T_i - T_a)] = \rho u_{\infty} H_v \quad (4-7)$$

Here T_i is the temperature at the water-oil interface which may be computed for any known regression rate u and depth below the surface z according to equation 2-2.

$$T_i = (T_b - T_a) e^{-\frac{u}{\alpha_o} z} + T_a \quad (4-8)$$

So at any oil thickness there are two equations, 4-7 and 4-8, and two unknowns, u and T_i . Analytical approaches to the solution are cumbersome so reliance on iterative techniques proves to be useful in solving for u . A burning rate is first assumed and used in equation 4-8. By substituting the computed T_i into 4-7 a new u is determined. This must be compared with the assumed value and if considerably different, be taken as the new assumed value for the second iteration. This approach was taken to make a lower bound determination for three fuels - heptane, kerosene and gas oil. It is considered a lower bound since α_w/α_o was taken to be 2.0; it is usually less than this. The results are plotted in Figure 4-2 with non-dimensional variables. Once T_i reaches 100°C the water at the interface



Thickness of oil layer, $\frac{\delta}{\delta_{\infty}}$
Influence of Water Sublayer on the Burning of Fuels

Figure 4-2

begins to boil and the heat transfer is no longer due to conduction alone. Gas oil reaches this point when $\delta/\delta_\infty = 1.69$ whereas heptane never reaches the point. Its boiling point is 98.5°C. Not only does the regression rate decrease when the oil layer becomes thinner, but its rate of decrease becomes greater.

When the water at the interface begins to boil, the temperature profile develops a more distinct discontinuity because now the interface temperature is fixed at 100°C. A proportion of the heat that now reaches the interface will be used to vaporize the water. This proportion increases as the oil layer becomes thinner. The remaining proportion is absorbed by the liquid water below the interface. Since the water surface is at constant temperature the change in temperature below the surface is governed by a relation $\sim \exp(z/\delta_\infty)^2$ instead of $\sim \exp(z/\delta_\infty)$ as before. For the time being the heat transfer to the water that this represents will be neglected since it is fairly small. Also, the thickness of the oil layer is on the order of one thermal length so the temperature distribution is approximately linear, specifically,

$$\frac{dT}{dz} = \frac{T_{bo} - T_{bw}}{\delta_i} \quad (4-9)$$

where δ_i is the thickness when $T_i = T_{bw}$, the boiling point of water. It can be obtained from a graph such as Figure 4-2 or computed directly by first computing u using equation 4-7 for $T_i = 100^\circ\text{C}$ and using that u to determine z or δ by:

$$\delta_i = \frac{\lambda}{\rho u c_p} \ln \left[\frac{T_{bo} - T_a}{T_i - T_a} \right] \quad (4-10)$$

The heat supplied to vaporize the water is approximated by taking the difference in heat transfer rates for two different thicknesses, namely, the original thickness and a thickness some time afterward.

$$q_w = \lambda (T_{bo} - T_{bw}) \left(\frac{1}{\delta} - \frac{1}{\delta_i} \right) \quad (4-11)$$

That heat which goes to the oil is the heat of vaporization plus a heat capacity term which is $1/2 c_{po} (T_{bo} - T_{bw})$, the result of a constant temperature drop across a decreasing thickness.

$$q_o = \rho u [h_v + 1/2 c_{po} (T_{bo} - T_{bw})] = \rho (h_v + 1/2 c_{po} \Delta T_b) \frac{d\delta}{dt} \quad (4-12)$$

Finally, utilizing the assumption of constant heat input,

$$q_{in} = q_o + q_w = \rho u_{\infty} H_v \quad (4-13)$$

More and more of the heat produced by burning goes to vaporize water as the oil layer becomes thinner. At the same time, u is decreasing. Eventually a point will be reached where the surface heat input is equal to that being absorbed by the boiling water. Then

$$q_w = q_{in} \quad \text{and} \quad u = \frac{d\delta}{dt} = 0$$

At this time there is no more oil vaporizing so there can be no flame -- the fire has been extinguished. Using equation 4-11 to compute the oil layer thickness at extinguishment results in:

$$\frac{\delta_{\text{ext}}}{\delta_i} = \frac{\lambda \Delta T_b}{\lambda \Delta T_b + \rho u_{\infty} H_v \delta_i} \quad (4-14)$$

The fuels with boiling points less than 100°C have no such extinguishment thickness, those with higher boiling points have a thickness which becomes greater with respect to the initial thickness as boiling point increases. Higher boiling point fuels also have a higher δ_i so the effect on the value of δ_{ext} is compounded. For instance, the computed extinguishing thickness for gas oil, whose boiling point is 240°C, is 0.15 cm, for kerosene it is 0.10 cm. This is shown in Figure 4-2.

The preceding development predicts a lower bound value for δ_{ext} since the heat transfer to the remaining liquid water was neglected. Accurate accounting of this factor must entail a time dependent solution. Such a solution is judged to be of limited usefulness since other effects will take place before the small change in the water's heat capacity becomes significant.

One of the first effects of a lower regression rate is the decrease in flame height that will occur as per equation 1-1. The assumption of constant heat input is a good assumption so long as the view factor and opacity factor in equation 1-2 remain constant. Should the height of the flames decrease to a point where the effective emissivity of the fire changes, the mass burning rate will fall off rapidly. Secondly,

where the fire at first had only the burnt air and fuel to raise to the steady state flame temperature, T_f , it must now also raise the temperature of the vaporized water. Although the specific heat of the water vapor is about twice that of the burnt gases its heat of vaporization is about ten times the oil's so the total mass of water evaporated is small in relation to the oil. The cooling of the flame from this effect is not especially important until the flame is nearly extinguished. Finally, there is a third cooling effect on the oil layer from the boiling water. The vaporized water at 100°C receives additional heat from the hotter oil layer as the water vapor bubbles pass through on the way to the surface. The heat lost in this fashion represents another small decrease in the burning rate.

3. Comparison with experimental results

There is at least one published experiment whose results may be used to verify the accuracy of this model. Maybourn [20] burned Kuwait crude oil on water in thicknesses of $1/8$ and $1/2$ inch. The tank was 80 square feet in area which is the equivalent of a diameter of 3 m. After ignition, the water began boiling under the $1/8$ " layer within 15 seconds, while it took $2\frac{1}{2}$ minutes before it occurred under the $1/2$ " layer. Total burning times were $1\frac{1}{4}$ minutes and 4 minutes respectively. About 15% of the material remained after flame extinguishment. From the data supplied for Kuwait crude in reference 20 it is possible to apply equations 4-10 and 4-14 and compute the approximate times to boiling and extinguishment based on the model. The comparative results are:

	1/8" (.318 cm)		1/2" (1.27 cm)	
	<u>Model</u>	<u>Experiment</u>	<u>Model</u>	<u>Experiment</u>
Time to boiling	30 sec	15 sec	4.25 min	2.5 min
Time to burn	1.5 min	1.25 min	5.75 min	4.0 min

The computed thickness of the oil at which water begins boiling is 0.4 cm and since the 1/8" layer is already thinner than this, boiling should theoretically begin immediately. The 15 second delay represents the transient heating which takes place from ignition until the interface temperature reaches 100°C. A theoretical transient time of 30 sec was obtained from Figure 22 in Ref. 7 which relates dimensionless time to dimensionless thickness. Boiling occurs earlier in the case of the 1/2" layer because the model has neglected the effect of the deeper heat penetration which exists in the burning of a binary mixture. Also, as the oil was heating up, only the lighter fractions were being burned and since their burning rates are higher than the average for the crude, the surface may have regressed farther than the model, which uses the average rate, would predict. This would shorten the burning time accordingly. The computed time from initiation of water boiling to burnout agrees reasonably well with the observed time in both experiments.

Chapter 5

Application of Model to Real Burns

Recent work in the field of burning oil spills has been centered around the use of "wicking agents" [18,21]. While successful burns have been accomplished with these agents, it is unclear exactly what the underlying mechanism might be. Hillstrom has experimented with activated charcoal which when mixed with decalin allowed its relatively thin layer to burn to completion. Similar tests were performed with kerosene and mineral oil. Since all of these substances have boiling points substantially above 100°C, the thickness of the oil layer at which water at the interface will start boiling is, according to results in Chapter 4, about 0.3 cm. The equilibrium thickness of the fuel lenses is not really this large and, in fact, sustained burning of waterborne kerosene or mineral oil above is difficult to achieve (although when hexane was added, some burns were successful) [18]. Adding charcoal to these oil layers made them thicker and in all cases Hillstrom was able to burn the original waterborne fuel layers to completion. The charcoal made the layers thick enough so that the burning surface was moved farther away from the water to a distance probably not too much different from what the analysis in Chapter 4 would predict. The analytical model also predicts that greater thicknesses of oil are required for oils with higher boiling temperature. In keeping with this trend, Hillstrom found it necessary to add a greater amount of

charcoal to the mineral oil than to the kerosene. Consequently, the higher boiling point mineral oil had a thickened thickness "much thicker" than the kerosene. As a topic for future research, it would be instructive to correlate the thicknesses of successfully burned charcoal-oil layers with the thicknesses that may be computed analytically in this work. If such a correlation can be made then it may reasonably be concluded that the major function of the charcoal is to provide insulation between the oil and the water.

The mechanism of burning when an agent such as charcoal is added is different from what occurs on an open surface. Tulley [21] attributes the success of his oil burns to the wicking action of his Cab-O-Sil but does not indicate how thick the burning layers were. A good indication of the similarity (or dissimilarity) of burns with wicking agents to those without could be obtained by comparing the flame heights of the fires with the agents to a computed flame height based on equation 1-1. The mass burning rate for equation 1-1 could be obtained from the regression rate data. If the flames were higher than the computed height it could be concluded that wicking in fact promotes faster burning than can be achieved in a continuous oil layer of considerable depth. If, however, the flame height is considerably smaller then it could be these "wicking agents" are playing a larger role as insulators to the water than they are by enhancing vaporization.

One further area of investigation that might be performed would be the analysis of fires whose burning rate is so much slower than

u_{∞} that the assumption of constant surface heat input is no longer valid. Hillstrom [18] and others [20] report that a flame will sustain itself so long as the fuel can be heated to some temperature above its flash point. In this type of burning the total heat required by the fuel is considerably less than what has been theorized by assuming the surface must remain at the boiling temperature, specifically, the difference in heat required would be:

$$q_{diff} = \rho u c_p (T_b - T_{fl}) \quad (5-1)$$

where T_{fl} is the flash point. A fire of this type cannot be expected to produce a great amount of heat since u will be small and fuel vaporized at the flash point will be able to combine with only the immediately available oxygen at the fuel surface. There can be no great amount of burning taking place at large distances from the surface since unlike the evolving of pure vapor from the boiling surface model, conditions are nearly stoichiometric upon vaporization. Vaporized fuel burns only a short distance above the surface. It is questionable whether equation 1-1 would apply to such a fire. Nevertheless, some fraction of heat is radiated back to the burning surface. So that now some fraction of heat from a smaller fire is being radiated to a fuel surface that requires proportionately less heat than if its surface were boiling. The amount of heat going to the water will depend on the temperatures of the interface which in turn is determined by the burning rate of the oil. Since it is small, the thermal thickness is large and the interface temperature will

be larger with respect to the surface temperature, T_{fl} . The determination to be made is whether this "flash point burning" is a reasonable model. If the balance between the greater proportion of available heat going to the water, the smaller amount required by the fuel, and the fraction of heat received at the surface from the small fire is favorable for burning then the model is plausible. The key to such an analysis is in knowing the amount of heat received by the surface. Presently available fire models have not dealt with fires of this character so it is still uncertain whether a "flash point" fire of burning oil can sustain itself atop water.

Conclusions

The analysis and models presented here as a result of this investigation are valid for making initial analytical determinations concerning the behavior of unconfined burning oil. More recent work in this field indicates that more sophisticated models may eventually be desired. However, any such models must take into account the results reported here in regard to thermal thicknesses and depths at which vaporization of water and/or oil might occur. It is seen that freely spreading oil nearly always maintains a thickness that is less than these theoretical thicknesses [13,16]. To achieve the thicknesses mandated by this model the oil cannot be allowed to spread indefinitely but should instead be inhibited in its travel by either physical or chemical barriers (booms or surface active agents or thickeners). The advantages of the thicker oil layer are obvious but include

- (1) The opportunity for faster burning rates
- (2) The decrease in the rate of evaporation of more volatile components
- (3) The decrease in emulsion activity with the water

In practice, of course, it may be physically impossible to contain spreading oil to any appreciable extent. To this end, solutions which will produce the same effect of increased oil thickness must be found.

For the present, however, the proposed modeling techniques in this work may be used to help determine what thicknesses and depths of fuel layers are important for any variety of oils in question. It

has been shown that,

(1) Complex oils may be approximated as binary solutions consisting of two components with different volatilities.

(2) The multicomponent nature of oils tends to extend the temperature profile in the uppermost layers so that vaporization of the more volatile component may be accommodated. The more diverse an oil's components are, the deeper will be this layer of vaporization activity.

(3) Water below the burning oil absorbs 3 to 4 times as much stored heat for every degree rise as does the liquid oil above.

(4) Heat absorption by the underlying water will slow the burning rate but not necessarily extinguish the fire. In cases where the water begins boiling the burning rate diminishes more rapidly and the fire will face extinguishment before all the oil is consumed. It is possible to estimate what the extinguishing oil thickness will be.

(5) Burning rates are relatively insensitive to the ambient oil temperatures. When oil is on top of water lower temperature may cause a decrease in the absolute burning rate but burning may actually be enhanced as a result of the greater oil thicknesses possible from the higher viscosities and surface tensions that will be present.

(6) Fuels with very high boiling points will require substantial thicknesses (~ 1 cm) if they are to be burned without the aid of "wicking agents".

Application of some of the data and developed results detailed herein will permit a more rational approach to the subject of burning oil on water.

Appendix A

Development of the Binary Boiling Curves

1. x_2 as a function of T

From equation 3-5,

$$x_2 = \frac{P_{1,0} - P_{atm}}{P_{1,0} - P_{2,0}} = \frac{1 - \frac{P_a}{P_{1,0}}}{1 - \frac{P_{2,0}}{P_{1,0}}} \quad (A-1)$$

Integrating equation 3-7 for any gas between a given pressure and atmospheric pressure gives:

$$\ln\left(\frac{P_a}{P}\right) = \frac{h_v M}{R} \left[\frac{1}{T} - \frac{1}{T_b} \right]$$

h_v = latent heat of vaporization

M = molecular weight

R = universal gas constant = $1.9859 \frac{\text{cal}}{\text{g mole} \cdot ^\circ\text{K}}$

T_b = absolute saturation (boiling) temperature at atmospheric pressure P_a

T = absolute saturation temperature at P

Then

$$\ln\left(\frac{P_a}{P_{1,0}}\right) = \frac{h_{v1} M_1}{R} \left[\frac{1}{T} - \frac{1}{T_{b1}} \right] \quad (A-2)$$

Since

$$\frac{P_{2,0}}{P_{1,0}} = \frac{P_{2,0}}{P_a} \times \frac{P_a}{P_{1,0}}$$

then

$$\ln\left(\frac{P_{2,0}}{P_{1,0}}\right) = \frac{h_{v2} M_2}{R} \left[\frac{1}{T_{b2}} - \frac{1}{T} \right] + \frac{h_{v1} M_1}{R} \left[\frac{1}{T} - \frac{1}{T_{b1}} \right] \quad (A-3)$$

By assuming $h_{v2}M_2 \sim h_{v1}M_1 \sim h_vM$ where h_vM can be taken as the average,

$$h_vM = 1/2 (h_{v1}M_1 + h_{v2}M_2)$$

A-3 can be written

$$\ln \frac{P_{2,o}}{P_{1,o}} = \frac{h_vM}{R} \left(\frac{1}{T_{b2}} - \frac{1}{T_{b1}} \right) \quad (A-4)$$

Substituting A-2 and A-4 into A-1 gives

$$x_2 = \frac{1 - \exp \left[\frac{h_vM}{R} \left(\frac{1}{T} - \frac{1}{T_{b1}} \right) \right]}{1 - \exp \left[\frac{h_vM}{R} \left(\frac{1}{T_{b2}} - \frac{1}{T_{b1}} \right) \right]}$$

The latent heat of vaporization can be computed by

$$h_v = \frac{\Delta S_v \bar{T}_b}{M} \quad (A-5)$$

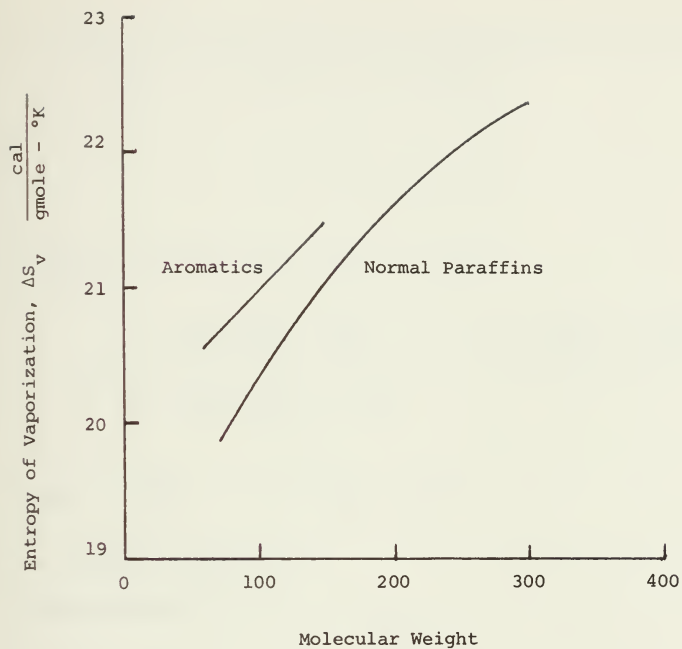
where ΔS_v is the entropy of vaporization, $\bar{T}_b = 1/2(T_{b1} + T_{b2})$.

Reference [13] gives an average value of ΔS_v as 20.5 cal/gmole °K

for most oils. More precise values may be obtained from Figure A-1.

Using equation A-5,

$$\frac{h_vM}{R} = \frac{\Delta S_v \bar{T}_b}{R}$$



Entropy of Vaporization

Figure A-1

By using what has been given as an average value for ΔS_v in Reference 13, a vaporization constant may be defined as

$$v = \frac{S_v}{R} = 10.3 \text{ } (^{\circ}\text{K})^{-2}$$

Now the final form of the equation becomes

$$x_2 = \frac{1 - \exp \left[v \bar{T}_b \left(\frac{1}{T} - \frac{1}{T_{b1}} \right) \right]}{1 - \exp \left[v \bar{T}_b \left(\frac{1}{T_{b2}} - \frac{1}{T_{b1}} \right) \right]} = \frac{1 - \exp \left[v \bar{T}_b \left(\frac{1}{T} - \frac{1}{T_{b1}} \right) \right]}{1 - P} \quad (\text{A-6})$$

$$\text{where } P = \frac{P_{2,o}}{P_{1,o}} = \exp v \bar{T}_b \left(\frac{1}{T_{b2}} - \frac{1}{T_{b1}} \right)$$

2. y_2 as a function of T

From equation 3-6

$$y_2 = \frac{P x_2}{1 + (P-1)x_2} \quad (\text{A-7})$$

Substituting A-6 for x_2

$$y_2 = \frac{P \left[1 - \exp v \bar{T}_b \left(\frac{1}{T} - \frac{1}{T_{b1}} \right) \right]}{1 + (P-1) \left[\frac{1 - \exp v \bar{T}_b \left(\frac{1}{T} - \frac{1}{T_{b1}} \right)}{1 - P} \right]}$$

Simplifying,

$$y_2 = \frac{P}{1-P} \left[\frac{1 - \exp \left[v \bar{T}_b \left(\frac{1}{T} - \frac{1}{T_{b1}} \right) \right]}{\exp \left[v \bar{T}_b \left(\frac{1}{T} - \frac{1}{T_{b1}} \right) \right]} \right] \quad (\text{A-8})$$

3. T as a function of x_2 and y_2

Solving for T in equations A-6 and A-8 gives

$$T = \left\{ \frac{1}{T_{b1}} + \frac{1}{vT_b} \ln \left[1 - x_2(1-P) \right] \right\}^{-1} \quad (\text{A-9})$$

$$T = \left\{ \frac{1}{T_{b1}} - \frac{1}{vT_b} \ln \left[1 + \frac{1-P}{P} y_2 \right] \right\}^{-1} \quad (\text{A-10})$$

All temperatures in the above expressions are in °K.

Appendix B

Determining the Depth at Which Boiling Begins in a Burning Binary Solution

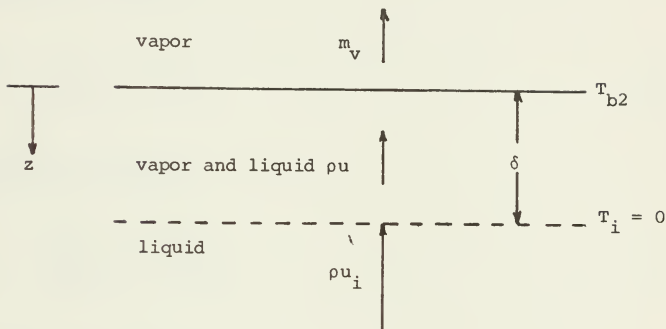


Figure B-1

Figure B-1 shows the system envisioned to determine where vaporization commences. Pure liquid crosses the lower boundary at the steady state mass burning rate. As it progresses to the free surface some of the lighter fractions are vaporized and the quantity ρu is correspondingly reduced by that amount vaporized. The gas given off rises through the remaining liquid and becomes heated to the surface temperature, here taken to be T_{b2} . The vapor generated closer to the surface contains more of the second component. The last bit to boil off is 100% second component.

In analyzing this system we require the equations for conservation of energy, continuity of mass and conservation of mass.

(1) Conservation of energy

$$\frac{d}{dz} \left(\lambda \frac{dT}{dz} + \rho u c_p T + \rho u c_{pv} (T_{bz} - T) \right) = m_v h_v \quad (B-1)$$

(2) Continuity of mass

$$\frac{d}{dz} (\rho u) = m_v \quad (B-2)$$

(3) Conservation of mass

$$\frac{d}{dz} (x_2 \rho u) = y_2 m_v \quad (B-3)$$

The boundary conditions are:

$$\begin{aligned} z = 0: & \quad \rho u = 0 & \quad T = T_{bz} - T_i \\ z = \delta: & \quad \rho u = \rho u_i & \quad T = T_i = 0 \end{aligned}$$

In the above equations,

λ = average thermal conductivity

ρ = average density

h_v = average heat of vaporization

u = linear burning rate

c_p = specific heat of liquid

c_{pv} = specific heat of vapor

m_v = mass rate of vapor evolution

x_2, y_2 = mole fractions of second component in the liquid and vapor, respectively

Substituting B-2 into B-1 and integrating from 0 to δ gives

$$\lambda \frac{dT}{dz} + \rho u (c_p T + c_{pv} (T_{b2} - T) - h_v) = - \rho u_k h_v \quad (B-4)$$

with the imposition of the boundary conditions, also let

$$\lambda \frac{dT}{dz} = g = [h_v (\rho u - \rho u_1) - \rho u c_p t - \rho u c_{pv} (T_{b2} - T)] \quad (B-5)$$

Substitution of B-2 into B-3 yields

$$\rho u \frac{dx_2}{dz} + x_2 \frac{d(\rho u)}{dz} = y_2 m_v \quad (B-6)$$

Further substitution gives

$$\rho u \frac{dx_2}{dz} + x_2 m_v = y_2 m_v$$

but

$$\frac{dx_2}{dz} = \frac{dx_2}{dT} \times \frac{dT}{dz}$$

so

$$\left(\rho u \frac{dx_2}{dT} \right) \frac{dT}{dz} = (y_2 - x_2) m_v \quad (B-7)$$

Solving for m_v ,

$$m_v = \frac{\rho u \frac{dx_2}{dT}}{y_2 - x_2} \frac{dT}{dz} \quad (B-8)$$

Also, by combining B-8 and B-2,

$$\frac{d}{dz} (\rho u) = \frac{\rho u \frac{dx_2}{dT}}{y_2 - x_2} \frac{dT}{dz} \quad (\text{B-9})$$

For constant density,

$$\frac{d}{dz} (\rho u) = \frac{du}{dz}$$

so B-10 becomes

$$\frac{du}{dT} = \frac{u \frac{dx_2}{dT}}{y_2 - x_2} dT$$

or

$$d \ln u = \frac{\frac{dx_2}{dT}}{y_2 - x_2} dT \quad (\text{B-10})$$

Integrating B-10,

$$\ln \frac{u}{u_i} = \frac{\frac{dx_2}{dT}}{y_2 - x_2} dT \quad (\text{B-11})$$

To permit the analytical integration of B-11 x_2 and y_2 will be approximated by linear functions

$$x_2 = 1 - S_x (T_{b2} - T)$$

$$y_2 = 1 - S_y (T_{b2} - T)$$

Now B-11 may be integrated as follows:

$$\ln \frac{u}{u_i} = \int_{T_i}^T \frac{\frac{S_x}{(S_x - S_y)(T_{b2} - T)}}{dT}$$

$$\frac{u}{u_i} = \left[\frac{T_{b2} - T}{T_{b2} - T_i} \right]^{\frac{S_x}{S_y - S_x}} \quad (\text{B-12})$$

Dividing B-5 by ρu_i and substituting B-12 gives

$$\frac{\lambda}{\rho u_i} \frac{dT}{dz} = \left[\frac{T_{b2} - T}{T_{b2} - T_i} \right]^{\frac{S_x}{S_y - S_x}} [h_v - c_{pv} T_{b2} + T(c_{pv} - c_p)] - h_v \quad (\text{B-13})$$

For an analytical solution to be performed the exponent $\frac{S_x}{S_y - S_x}$ must be unity. Linear approximations of x_2 and y_2 generally give a value for the slopes which will result in an exponent of one. Expanding B-13 for $\frac{S_x}{S_y - S_x} = 1$, $T_i = 0$,

$$\frac{\lambda}{\rho u_i} \frac{dT}{dz} = T^2 \frac{(c_p - c_{pv})}{T_{b2}} + T \left(2c_{pv} - c_p - \frac{h_v}{T_{b2}} \right) - c_{pv} T_{b2} \quad (\text{B-14})$$

Since the right hand side is quadratic in T , let

$$a = \frac{c_p - c_{pv}}{T_{b2}} \quad c = -c_{pv} T_{b2}$$

$$b = 2c_{pv} - c_p - \frac{h_v}{T_{b2}} \quad Q = b^2 - 4ac$$

Equation B-14 takes the form of:

$$dz = \frac{\lambda}{\rho u_i} \frac{dT}{aT^2 + bT + c} \quad (\text{B-15})$$

Integrating from 0 (the surface) to δ on the left hand side and T_{b2} to T on the right hand side gives the result

$$\delta = \frac{2\lambda}{\rho u_i \sqrt{Q}} \left[\tanh^{-1} \frac{2aT_{b2} + b}{\sqrt{Q}} - \tanh^{-1} \frac{2aT + b}{\sqrt{Q}} \right] \quad (\text{B-16})$$

The choice of T will depend on the original composition of the liquid. Generally, $T \approx T_i$.

Pertinent Properties of Some Petroleum Products

Substance	ρ @ 15°C $\frac{\text{g}}{\text{cm}^3}$	Boiling Point °C	h_v @ B.P. $\frac{\text{cal}}{\text{g}}$	$\lambda \times 10^3$ $\frac{\text{cal}}{\text{cm-sec-}^\circ\text{C}}$	C_p $\frac{\text{cal}}{\text{g-}^\circ\text{C}}$
Butane	0.579	-0.5	92.1		0.550
Pentane	0.631	36.0	85.4	0.3221	0.565
Hexane	0.664	68.7	80.0	0.3287	0.600
Petroleum ether	0.666		84.0		
Heptane	0.688	98.4	75.6	0.3354	0.590
Octane	0.706	125.7	72.0	0.3469	0.578
Ethyl ether	0.714	34.6	82.4	0.3283	
Nonane	0.721	150.8	68.8	0.3374	0.503
Decane	0.733	174.1	66.0	0.3349	0.502
Gasoline	0.74	136	80		
Undecane	0.744	195.9	63.5		0.501
Tridecane	0.756	235.4	59.2		0.498
Naptha	0.787		69.0		
Acetane	0.792		69.4	0.4192	0.458
Ethanol	0.794	78.3	263.3	0.3995	0.581
Kerosene	0.810	205	58.0	0.5	0.5
Butanol	0.814	117.7	141.1	0.3663	0.563
Isoamyl alcohol	0.815	102.2	120	0.3531	0.535
Amyl alcohol	0.819	130	123.9	0.3874	0.712
Gas oil	0.823	240	59		0.49
m-Xylene	0.868	138.4	81.2	0.3767	0.397
Toluene	0.871	110.6	86.8	0.2808	0.490
Benzene	0.879	80.1	94.1	0.3439	0.435
Heavy fuel oil	0.99	320	48		0.45

Appendix D

Tabulation of Some Fractionation Data

Substance	$\frac{g}{cm^3}$	Distilled Spirits					End Point
		Density	Initial Boiling Point	10%	50%	90%	
Natural gasoline	0.671			42.8	64.4	113.3	157.8
Aviation gasoline	0.724		42.0				169.0
Straight-run gasoline	0.729				64.4	168.9	186.1
Motor gasoline	0.733		37.0				185.0
JP-2	0.756			69.4		221.1	258.3
JP-4	0.768			98.3		215.0	245.0
Naptha	0.787		54.0			238.0	276.0
No. 1 grade kerosene	0.811		175.0	194.4	220.6		278.3
JP-1	0.815			173.9	192.2	225.0	
JP-5	0.822			198.9	216.1	241.1	263.3
Vaporizing oil	0.823		145.0		196.0		266.0
No. 1 fuel oil	0.825			205.0	232.0	263.0	279.0
No. 2 grade kerosene	0.849		183.9	220.6	261.1		334.4
No. 2 fuel oil	0.857			226.0	265.0	315.0	340.0
No. 4 Residual (typical)				270.6	322.8	548.3	
No. 5 fuel oil	0.935			<315		>371	
No. 6 fuel oil	0.998			345	475		

List of Symbols

a	Constant used in Appendix B
b	Constant used in Appendix B
c	Constant used in Appendix B
c_p	Specific heat, cal/g-°C
d	Diameter, pool or tank, cm
e	Base of natural logarithms, 2.718...
F	View factor
F_s	Spreading coefficient, dyne/cm
g	Acceleration of gravity, 980 cm/sec ²
H_c	Net heat of combustion, cal/g
H_v	Sensible heat of vaporization, cal/g
h_v	Latent heat of vaporization, cal/g
K_r	Empirical constant
k	Constant, as defined
k_c	Constant, u/α_e , cm ⁻¹
L	Flame length, cm
M	Molecular weight
MF	Mole fraction
m	Mass burning rate g/cm ² -sec and g/cm ² -min
p	pressure, mm Hg
Q	Constant used in Appendix B
q	Heat flux cal/cm ² -sec
q_{in}	Heat flux to free surface cal/cm ² -sec

q_s	Same as q_{in}
R	Universal gas constant, 1.9859 cal/g mole - $^{\circ}K$
r	Radius, cm
ΔS_v	Entropy of vaporization, cal/g mole - $^{\circ}K$
T	Temperature, $^{\circ}C$ and $^{\circ}K$
T_a	Ambient temperature, $^{\circ}C$
T_b	Boiling temperature, $^{\circ}C$
T_f	Flame temperature, $^{\circ}C$
T_{fl}	Flash point, $^{\circ}C$
T_i	Initial temperature, Chapter 3, $^{\circ}C$
$T_{i\omega}$	Water-oil interface temperature, Chapter 4, $^{\circ}C$
t	Time, sec
δ	Wall thickness, Chapter 2, cm
U	Convection heat transfer coefficient, cal/cm ² -sec
u	Linear burning rate, cm/min, mm/min and cm/sec
VF	Volume fraction
v	Volume, cm ³
x	Mole fraction in liquid
y	Mole fraction in vapor
z	Depth in vertical direction, positive downward, cm
α	Thermal diffusivity, cm ² /sec
α_e	Effective thermal diffusivity, cm ² /sec
β	Coefficient of volume expansion, $^{\circ}C^{-1}$
δ	Oil thickness in z direction
δ_{ext}	Oil thickness at flame extinguishment

κ	Constant relating to emissivity, cm^{-1}
λ	Thermal conductivity, $\text{cal/cm-sec-}^{\circ}\text{C}$
λ_s	Steel thermal conductivity, $\text{cal/cm-sec-}^{\circ}\text{C}$
π	Constant, 3.14159...
ρ	Density, g/cm^3
ρ_a	Air density, g/cm^3
σ	Surface tension, dyne/cm except Chapter 1
σ	Stefan-Boltzmann constant, Chapter 1, $1.354 \times 10^{-12} \text{ cal/cm}^2\text{-sec-}^{\circ}\text{K}$

Subscripts

eq	Refers to equilibrium conditions
i	Refers to initial conditions (interface in Chapter 4)
o	Refers to oil except Chapter 3
o	Refers to original conditions, Chapter 3
s	Refers to surface conditions, Chapter 3
t	At some time
v	Refers to vapor
w	Refers to water
1	Refers to the lighter component
2	Refers to the heavier component

References

1. Thomas, P.H., "The Size of Flames from Natural Fires." Ninth Symposium (International) on Combustion, Academic Press, New York, 1963. p. 844-859.
2. Blinov, V.I. and Khudyakov, G.N., "Certain Laws Governing the Diffusive Burning of Liquids," Academia Nauk, SSSR Doklady, 113, 1094-1098 (1957). Reviewed by Hottel, H.C., Fire Research Abstracts and Reviews, 1, 41-44 (1959).
3. Burgess, D. and Hertzberg, M., "Radiation from Pool Fires," Heat Transfer in Flames, John Wiley & Sons, 1974.
4. Blinov, V.I. and Khudyakov, G.N., Diffusion Burning of Liquids. Izdatel'stvo Akademii Nauk SSSR, 1961. Tr. by Research Information Service for U.S. Army Engineer Research and Development Laboratories, Fort Belvoir, Va., 1964.
5. Emmons, H.W., "Some Observations on Pool Burning," International Symposium on the Use of Models in Fire Research. National Academy of Sciences, National Research Council, Pub. 786, 1961.
6. Rasbash, D.J., Rogowski, Z.W. and Stark, G.W.V., "Properties of Fires of Liquids," Fuel, 35, p. 94-107, 1956.
7. Tarifa, C.S., "Open Fires and Transport of Firebrands," Instituto Nacional de Tecnica Aeronautica "Esteban Terradas", Madrid, Spain, 31 May 1962-31 May 1963.
8. Burgoyne, J. and Katan, L., "Burning of Petroleum Products in Open Tanks," Journal of the Institution of Petroleum Technologists, 33, 158 (1947).
9. Zeitfuchs, E.H., "Specific Heats, Heats of Vaporization, and Critical Temperatures of California Petroleum Oils," Industrial & Engineering Chemistry, 18, 79-82 (1926).
10. Guthrie, V.B. ed., Petroleum Products Handbook. McGraw-Hill Book Co., 1960.
11. Brown, G.G., Katz, D.L., Oberfell, G.G. and Alden, R.C., Natural Gasoline and the Volatile Hydrocarbons. Natural Gasoline Association of America, 1948.
12. Rossini, F.D., Selected Values of Physical and Thermodynamic Properties of Hydrocarbons and Related Compounds. Carnegie Press for the American Petroleum Institute, 1953.

13. Blokker, P.C., "Spreading and Evaporation of Petroleum Products on Water," Proceedings of the 4th International Harbour Conference, Antwerp, 1964, p. 911-919.
14. Fay, J.A., "Physical Processes in the Spread of Oil on a Water Surface," from Joint Conference on Prevention and Control of Oil Spills, June 15-17, 1971.
15. Fay, J.A., "The Spread of Oil Slicks on a Calm Sea," from Oil on the Sea, May 1969.
16. Berridge, S.A., Dean, R.A., Fallows, R.G. and Fish, A., "The Properties of Persistent Oils at Sea," Institute of Petroleum Journal 54, 300-309 (1968).
17. Smith, D.L. and MacIntyre, W.G., "Initial Aging of Fuel Oil Films of Sea Water," Joint Conference on Prevention and Control of Oil Spills, June 15-17, 1971, Washington, D.C. p. 457-461.
18. Hillstrom, W.W., "Ignition and Combustion of Unconfined Liquid Fuels," Combustion Science and Technology, 3, 179-186 (1971).
19. Baumeister, T., ed., Standard Handbook for Mechanical Engineers. McGraw-Hill Book Co., 1967.
20. Maybourn, R., "The Work of the IP Working Group on the Burning of Oil," Institute of Petroleum Journal, 57, 12-16 (1971).
21. Tully, P.R., "Removal of Floating Oil Slicks by the Controlled Combustion Technique," Hoult, D.P., ed., Oil on the Sea, Proceedings of a Symposium on the Scientific and Engineering Aspects of Oil Pollution of the Sea, May 16, 1969, Cambridge, Mass. p. 81-91.
22. Freiburger, A. and Byers, J.M., "Burning Agents for Oil Spill Cleanup." 1971 Joint Oil Spill Conference Proceedings, Washington, C.C.

Bibliography

1. Bland, W.F. and Davidson, R.L. ed., Petroleum Processing Handbook. McGraw-Hill Book Co., 1967.
2. Guthrie, V.B. ed., Petroleum Products Handbook. McGraw-Hill Book Co., 1960.
3. Maxwell, J.B., Data Book on Hydrocarbons. D. Van Nostrand, Co., Inc., 1950.
4. Brown, G.G., Katz, D.L., Oberfell, G.G. and Alden, R.C., Natural Gasoline and the Volatile Hydrocarbons. Natural Gasoline Association of America, 1948.
5. Spiers, H.M., ed., Technical Data on Fuel. The British National Committee, World Power Conference, 1961
6. Rossini, F.D., Selected Values of Physical and Thermodynamic Properties of Hydrocarbons and Related Compounds. Carnegie Press for the American Petroleum Institute, 1953.
7. Baumeister, T., ed., Standard Handbook for Mechanical Engineers. McGraw-Hill Book Co., 1967.
8. Hodgman, C.D., ed., Handbook of Chemistry and Physics. Chemical Rubber Publishing Co., 1958.
9. Symposium on Composition of Petroleum Oils, Determination and Evaluation. ASTM Special Publication No. 224, 1958.
10. Hottel, H.C. and Sarofim, A.F., Radiative Transfer. McGraw-Hill Book Co., 1967.
11. Siegel, R. and Howell, J.R., Thermal Radiation Heat Transfer. McGraw-Hill Book Co., 1972.
12. Afgan, N.H. and Beer, J.M. ed., Heat Transfer in Flames. John Wiley & Sons, 1974.
13. Blackshear, P.L. ed., Heat Transfer in Fires: Thermophysics, Social Aspects, Economic Impact. John Wiley & Sons, 1974.
14. Gaydon, A.G. and Wolfhard, H.G., Flames: Their Structure, Radiation and Temperature. Chapman & Hall, London, 1970.
15. Berl, W.G. ed., International Symposium on the Use of Models in Fire Research. National Academy of Sciences, National Research Council, Pub. 786, 1961.

16. Burgess, D. and Hertzberg, M., "Radiation from Pool Fires," From Ref. 12.
17. Blinov, V.I. and Khudiakov, G.N., "Certain Laws Governing the Diffusive Burning of Liquids," Academiia Nauk, SSSR Doklady, 113, 1094-1098 (1957). Reviewed by Hottel, H.C., Fire Research Abstracts and Reviews, 1, 41-44 (1959).
18. Blinov, V.I. and Khudyakov, G.N., Diffusion Burning of Liquids. Izdatat'stvo Akademii Nauk SSSR, 1961. Tr. by Research Information Service for U.S. Army Engineer Research and Development Laboratories, Fort Belvoir, Va., 1964.
19. Emmons, H.W., "Some Observations on Pool Burning," From Ref. 15.
20. Rinsinger, J.L., "How Oil Acts When it Burns," Petroleum Refiner, 36, p. 114-116, 259-262, Jan. 1957.
21. Rasbash, D.J., Rogowski, Z.W. and Stark, G.W.V., "Properties of Fires of Liquids," Fuel, 35, p. 94-107, 1956.
22. Seeger, P.G., "On the Combustion and Heat Transfer in Fires of Liquid Fuels in Tanks," From Ref. 13.
23. Corlett, R.C., "Interactions Between Flames and Condensed Phase Matter," from Ref. 13.
24. Corlett, R.C., "Concentration and Temperature Similarity," from Ref. 13.
25. Kelly, C.S., "The Transfer of Radiation from a Flame to its Fuel," Journal of Fire and Flammability, 4, 56-66. (1973).
26. Lee, C.K., "Estimates of Luminous Flame Radiation from Fires," Combustion and Flame, 24, 239-244 (1975).
27. Burgess, D.S., Grumer, J. and Wolfhard, H.G., "Burning Rates in Liquid Fuels in Large and Small Open Trays," From Ref. 15.
28. Burgoyne, J. and Katan, L., "Burning of Petroleum Products in Open Tanks," Journal of the Institution of Petroleum Technologists, 33, 158 (1947).
29. Tarifa, C.S., "Open Fires and Transport of Firebrands," Instituto Nacional de Tecnica Aeronautica "Esteban Terradas", Madrid, Spain, 31 May 1962-31 May 1963.
30. Huffman, K.G., Welker, J.R. and Sliepcevich, C.M., "Interaction Effects of Multiple Pool Fires," Fire Technology, 5, 225-232 (1969).

31. Burgess, D., Strasser, A. and Grumer, J., "Diffusive Burning of Liquid Fuels in Open Trays," Fire Research Abstracts and Reviews, 3, 177 (1961).
32. Arnold, J.H., "Estimation of Latent Heats of Vaporization," Industrial & Engineering Chemistry, 25, 659 (1933).
33. Weir and Easton, "Heat Content of Petroleum Oil Fractions at Elevated Temperatures," Industrial & Engineering Chemistry, 24, 210 (1932).
34. Zeitfuchs, E.H., "Specific Heats, Heats of Vaporization, and Critical Temperatures of California Petroleum Oils," Industrial & Engineering Chemistry, 18, 79-82 (1926).
35. Lang, H.R. and Jessel, R., "The Total Heat and Specific Heat of a Series of Fractions of Petroleum Oil, and Their Relation to Other Properties," Journal of the Institution of Petroleum Technologists, 17, 572 (1931).
36. Nakakuki, A., "Blow-off and Flame Spread in Liquid Fires," Combustion Science & Technology, 9, 71-73 (1974).
37. Torrance, K.E., "Subsurface Flows Preceding Flame Spread Over a Liquid Fuel," Combustion Science & Technology, 3, 133-143 (1971).
38. Tully, P.R., "Removal of Floating Oil Slicks by the Controlled Combustion Technique," Hoult, D.P., ed., Oil on the Sea, Proceedings of a Symposium on the Scientific and Engineering Aspects of Oil Pollution of the Sea, May 16, 1969, Cambridge, Mass. p. 81-91.
39. Smith, C.L. and MacIntyre, W.G., "Initial Aging of Fuel Oil Films of Sea Water," Joint Conference on Prevention and Control of Oil Spills, June 15-17, 1971, Washington, D.C. p. 457-461.
40. Fay, J.A., "Physical Processes in the Spread of Oil on a Water Surface," From Ref. 39, p. 463-467.
41. Fay, J.A., "The Spread of Oil Slicks on a Calm Sea," From Ref. 38, p. 53-64.
42. Blokker, P.C., "Spreading and Evaporation of Petroleum Products on Water," Proceedings of the 4th International Harbour Conference, Antwerp, 1964, p. 911-919.
43. Berridge, S.A., Dean, R.A., Fallows, R.G. and Fish, A., "The Properties of Persistent Oils at Sea," Institute of Petroleum Journal 54, 300-309 (1968).

44. Hillstrom, W.W., "Ignition and Combustion of Unconfined Liquid Fuels," Combustion Science and Technology, 3, 179-186(1971).
45. Maybourn, R., "The Work of the IP Working Group on the Burning of Oil," Institute of Petroleum Journal, 57, 12-16, (1971).
46. Adler, J., "Fluid Mechanics of a Shallow Fuel Layer Near a Burning Wick," Combustion Science & Technology, 2, 105 (1970).
47. Directory of Fire Research in the U.S., 6th Ed. (1969-1971), 7th ed. (1971-1973).
48. Thomas, P.H., "The Size of Flames from Natural Fires," Ninth Symposium (International) on Combustion, Academic Press, New York, 1963. p. 844-859.
49. Freiburger, A. and Byers, J.M., "Burning Agents for Oil Spill Cleanup." 1971 Joint Oil Spill Conference Proceedings, Washington, D.C.

Thesis
A563

Anthony

Modeling of burning
oil on a water surface.

171163

2 NOV 77

DISPLAY

Thesis
A563

Anthony

Modeling of burning
oil on a water surface.

171163

thesA563

Modeling of burning oil on a water surfa



3 2768 001 91545 7
DUDLEY KNOX LIBRARY